Worcester Polytechnic Institute

INTERACTIVE QUALIFYING PROJECT

An analysis of thermal energy storage solutions for Worcester Polytechnic Institute

Abstract

Increased reliance on renewable sources requires the implementation of efficient and cost effective energy storage solutions. An extensive meta-analysis is carried out in order to design a possible latent heat thermal energy storage device for meeting the energy storage needs of a university or similar sized institution requiring 1 MWh daily, with Worcester Polytechnic Institute used as the test case. A computer simulation, literature review and analysis of consumer energy data were made in order to reach conclusions regarding this technology and its performance against large scale lithium-ion batteries. Possible construction materials and market opportunities are also discussed in detail. Results show that the proposed thermal energy storage design using KNO_3 is severely limited by poor energy conversion efficiency, and that it is not practical unless the dissipated heat can be also be used.

Faculty Advisor
Powell, Adam C.

Authors
Koethe, Douglas
LaCroce, Tyler
Poggioli, Federico
Shahabuddin, Muntasir

Worcester, Massachusetts, US.

March 6, 2020

ACKNOWLEDGEMENTS

We would like to thank our advisor Adam Powell for his invaluable support as mentor, and always provide us with resources and suggestions for the project. We would also like to thank David Dussault for his help on designing the proposed Thermal Energy Storage Unit IQP. Finally, we thank the WPI Facilities team for providing the necessary energy data needed for the market analysis section of this project.

EXECUTIVE SUMMARY

<u>Introduction</u>

Movement towards intermittent renewable energy sources such as wind and solar power has created a greater need for energy storage to smooth supply availability and account for periods of scarce energy production. Development of storage systems to fill multiple niches is necessary. Thermal energy storage (TES) has been researched as a potential competitor to the current leading technology in utility-scale energy storage: lithium-ion electrochemical batteries.

The objective of this investigation is to evaluate the possibility of implementing a Thermal Energy Storage Unit (TESU) in order to satisfy the energy needs of a small population. For this we use Worcester Polytechnic Institute, a 6,600 student university in the New England area as a case study. A meta-analysis is conducted in order to evaluate possible thermal heat transfer mechanisms, energy conversion methods, and insulation technologies in order to design an optimal thermal energy storage unit for this purpose.

As a result, this project is split into two sections. First, an analysis of possible materials to be used in thermal energy storage units, including insulation and phase change materials, will be combined into a model to calculate relevant parameters for thermal energy storage units. Second, a market analysis of our modeled thermal energy storage unit will be compared against the current leading energy storage technology, lithium-ion.

<u>Findings</u>

TESM Selection

The main component for latent heat thermal energy storage is the phase change material (PCM). Analysis of PCMs considered for TES across multiple papers are considered to determine the most cost effective material in terms of heat of fusion. A good thermal energy storage material (TESM) has a large unit cost, capacity, and volume, and it has a higher heat of fusion that allows for more latent energy storage per unit mass.

A good TESM is paramount for unit cost, capacity, and volume, and a higher heat of fusion allows for more latent energy storage per unit mass. We found potassium nitrate (KNO_3) to be the most cost effective material. While it may have a relatively expensive price, it has a significantly higher heat of fusion of 266 kJ/kg as well as a higher melting point which makes it cost efficient relative to other TESMs. Additionally, it is an energy dense TESM option with appropriate melting points for steam generation and energy conversion.

Insulation

As is common, the best insulation is heavily dependent on context. Cost, system volume, pricing model, and container surface area are all relevant in determining how long energy needs to be stored for, the service temperatures of the insulation, cost of insulation, and amount of insulation needed for system capacity. In an ideal scenario, high temperature aerogel blankets surrounding a concrete vessel create the most effective insulation, but given the low production velocity and scale of high temperature aerogel solutions, ceramic fiber is an economic, realistic, and our recommended alternative given its significant edge price-wise, and similarly low thermal conductivity. Our premier options for insulation materials are tabulated below.

Classification	**Material**	**Continuous Use Temp (deg C)**	**Maximum Service Temp (deg C)**	**Temp ranges for Corresponding Material Properties (deg C)**	**Thermal Conductivity (W/(m*k))**	**Cost ($/m^3)**
Refractory Concrete	Kast-o-Lite 22 PLUS	815	1205	205	0.25	5626.69
Aerogel Blanket	Pyrogel XTE	600	650	200	0.028	51964
Ceramic Fiber	Cerachrom	1370	1427	260	0.06	35777.39
Firebrick	K-23 Firebrick	1704	1915	260	0.17	43420.49

Table 1. Insulation Material Comparison

Modeling Findings

A computer program was elaborated in order to accurately simulate the operation of the device. The software Mathematica was chosen due to its simple syntax and ability to handle operations involving a high level of abstraction with ease. The purpose of the program was to accurately calculate the heat flow rate between the PCM and its surroundings, both to the water inside the inner tank pipe and to air in the outer surface of the tank.

From the results obtained we believe that in order to produce 1MW of power output for 1 hour, about 33,835 kg of KNO_3 is required. The efficiency of the turbine was assumed to be 40%. This is assuming the device only operates using the amount of heat stored as latent heat, and a temperature drop of about 50 ^oC in the turbine. The results of the simulation can be seen on Figure 3, which shows the initial and final water temperature distributions of the water as the device is put into charging mode and the water starts to heat up. Results from the model show that during 60 minutes the water heats up from 373 K (100 ^oC, boiling temperature of water) to 607 K. (the upper temperature limit is 607 K = 334 ^oC, the PCM phase transition temperature) The change of the properties of water as temperature increases and the decrease in temperature difference between the PCM and steam explains the observed nonlinearity of the graph.

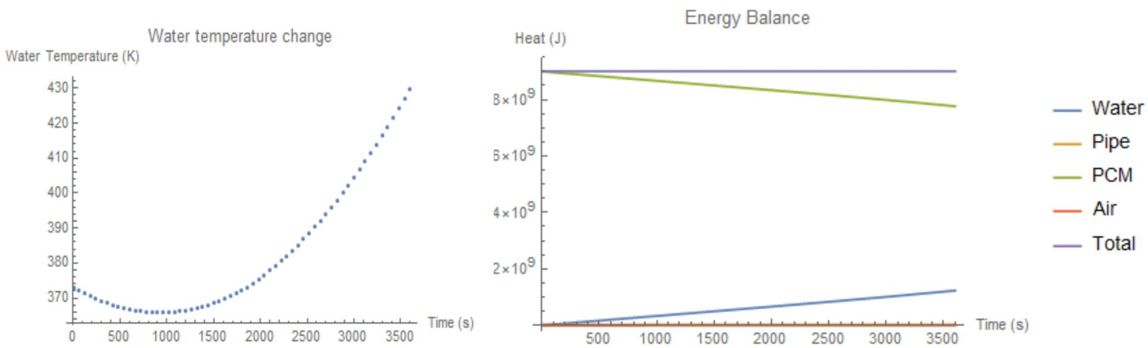

Figure 1. Water temperature and Energy balance graphs. (See note on Appendix A)

The amount of heat stored in the PCM tank at the beginning of the discharge cycle is 2.5 MWh ($9\ 10^9$ J). On the energy balance graph, the purple line represents the total energy of the system, while the green one refers to the amount of latent heat stored in the PCM Tank. The blue, yellow and red lines correspond to the heat being transferred to the water, air and the metal surface of the tank itself, respectively.

It is possible to conclude from the modeling of the thermal battery that this type of model is unlikely to be efficient enough to be implemented as a reliable TES device, unless the heat lost in electricity generation is repurposed for heating of WPI campus buildings. Although the model is limited by turbine conversion efficiency, the heat loss in properly insulated TES units undercuts that of lithium-ion. It is worth noting however, that our model accounts for only ideal insulation conditions--thermal bridging effects, which may play a major role in TES heat loss to the atmosphere, are not accounted for. Under our model, TES heat loss to the atmosphere is limited and serves to sell it as an attractive storage option, particularly given the lack of PCM degradation relative to lithium-ion chemistry. Figure 2 indicates the percentage heat loss per hour associated with different insulation thicknesses with an average thermal conductivity of 0.1 W/(m K).

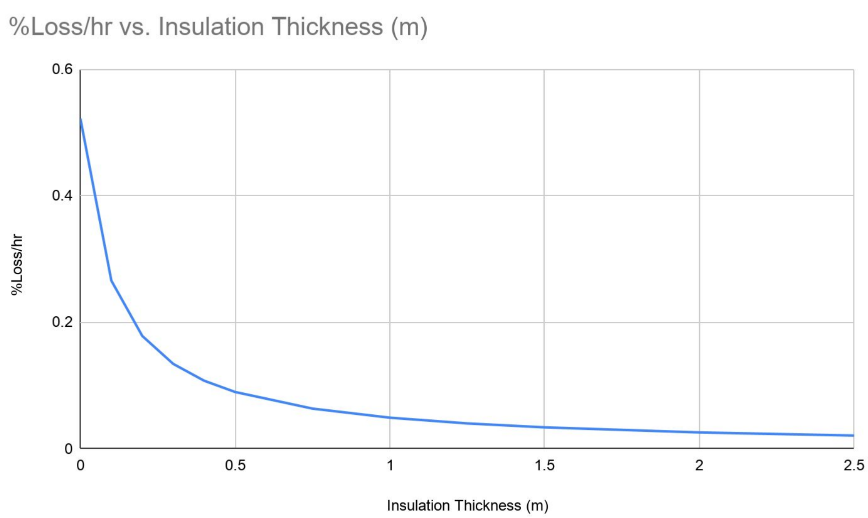

Figure 2. Percentage of heat loss per hour versus insulation thickness

Fixed off-peak/peak Market Analysis

Currently, energy storage is an expensive endeavor. Our models compare 1 MWh of effective storage in our modeled thermal energy storage as well as the current lithium-ion storage. We based our first analysis on National Grid's peak/off-peak pricing models rather than traditional peak shaving models to minimize loss due to length of storage time. Because of National Grid's set peak/off-peak hours of 8:00am to 9:00pm for peak hours and 9:00pm to 8:00am for off peak hours, charging times are set to be as soon as possible before the pricing switch at 8:00am, and discharge times are set to be the same after the pricing switch at 8:00am. Assuming a charge and discharge rate matching WPI's consumption at the respective times, this aims to limit energy loss in our modeled thermal battery, although this also limits a negligible amount of loss in lithium-ion batteries as well. Profit was measured as a simple net revenues minus costs fashion--where revenues include credits for energy sold at peak pricing periods, and costs include energy bought during off-peak hours and energy depreciation from loss parameters of each unit.

Following National Grid's pricing model and WPI's consumption data over 4 months--January, April, July, and October--each representing winter, spring, summer, and fall respectively--TES falls significantly short of profit in each month, while lithium-ion--while still falling short--results in very little loss, but loss nonetheless.

	January	**April**	**July**	**October**
Average Thermal Profit Per Day ($/day)	-61.42	-61.40	-61.38	-61.37
Average lithium-ion Profit Per Day ($/day)	-0.77	-0.77	-0.77	-0.77

Table 2. Average Energy Storage Profit per Season

Averaging losses around $75 per day places TES in a spot where significant design overhauls involving conversion efficiency improvement are required. Because lithium-ion's average profit loss is under a dollar per day, a battery with slightly higher efficiency could reach break-even or profit. However, since the 85% efficiency we assumed for lithium-ion is only 5% off from the current peak for lithium-ion of 90% efficiency, possible profits would be very limited and given that lithium-ion's investment cost is currently the limiting factor in its use, we advise against WPI using either of these technologies for peak shaving under National Grid's fixed off-peak/peak pricing models.

RTEP Findings

Real-time pricing is a more robust model for electricity pricing as dependence on intermittent renewables increases. We utilized the real time pricing the New England Independent System Operator (NE ISO) provides on their website, which is updated every 5 minutes, rather than National Grid's fixed price and fixed time pricing changes. To justify our recommendations, we assumed the most ideal scenario to determine possible efficiencies for profit. We determined the average peak and average trough prices, and took the ratio between the trough and peak prices. The ratio between the two prices indicates the minimum efficiency required for break-even assuming the prices are fixed at the peak price during peak hours, and the trough price during off-peak hours, similar to the National Grid model.

	January	April	July	October
Peak Price ($/kWh)	0.1097	0.0767	0.0792	0.0672
Trough Price ($/kWh)	0.0751	0.0587	0.0554	0.0522
Trough/Peak Price Ratio	0.685	0.766	0.699	0.777

Table 3. Peak/Trough Price Ratio per Season

As seen in across all months, the average trough/peak price ratios do not drop below 0.685, which correlates to a minimum battery efficiency for profit of 68.5% in the most ideal pricing scenario. Even with the largest price disparities over the day, our modeled thermal battery's efficiency of 40% will still result in significant loss each day if used for peak shaving--and this is not accounting for the (although marginal) additional heat loss to the atmosphere due to longer storage periods between the peak and trough prices. Under lithium-ion's projected efficiency range of 80-90% (or our calculated 76%), these trough/peak price ratios do indicate possible profit. However, because we are assuming the absolute ideal pricing scenario, and the required efficiencies are close to true lithium-ion efficiency, in the majority of true real time pricing situations, lithium-ion fares similarly to thermal on WPI's scale, albeit with lower loss. Our modeling indicates that both lithium-ion batteries and TES require either settings with lower trough/peak price ratios, or improvements in efficiency, in order to be competitive-- both of which may change across climates/regions and as use of renewables becomes more ubiquitous.

Heat Recycling

Heat recycling poises TES as a potentially genuinely useful technology. While all other market analyses point to TES leading to significant losses, the use of heat recycling to heat campus buildings vastly increases the efficiency of TES units when it is relevant. In the context of the colder months, heat recycling is a useful second use of the energy storage unit. With perfect utilization of heat recycling, the TES unit's efficiency can theoretically reach 100%. Although unrealistic, even 50% utilization of lost energy in heat recycling places TES's efficiency around 70%, nearing lithium-ion's efficiency. 75% heat recycling utilization places TES's efficiency at 85.5%, exactly in the range as the most efficient lithium-ion units. If utilized properly, heat recycling leaves TES in a favorable position economically. It is also a significantly greener source of heating, as the original heat source comes from electrically resistive heating, which bypasses the need for natural gas combustion, a common fuel source for heating systems at WPI, and parallels WPI's current plans for a gas cogeneration plant.

Lithium ion

Thermal energy storage fills niche roles when compared to lithium ion. Thermal energy is not viable for any small power or small scale applications. Yet, since lithium ion has a few key failing points, thermal energy storage can beat lithium ion in a few niche categories, particularly when thermal is used as a co-storage/heating unit and heat recycling increases its efficiency. When done over a larger scale, thermal energy is more viable. Additionally, lithium-ion has potential chemical failure at high amperage and high temperatures. Due to this fact, thermal energy storage is able to create a market in these two areas because lithium-ion cannot compare under these specific circumstances. Over multiple cycles, lithium-ion is also shown to exhibit degradation in capacity--but because TES only involves physical state changes, its cycle life is significantly higher, requiring only maintenance over time, rather than full replacements. lithium-ion provides a safer, more efficient storage method over TES currently. However, as TES develops, it is realistic to say the two will complement each other's weaknesses in scale, lifetime, investment cost, and storage cost.

Conclusion

The basic concept of using alternative methods of storing energy to make use of the real time energy production price method or provided alternative solutions to storing energy is an area that will continue to see major development. The specific method of thermal energy storage though, has a large number of efficiency and energy reclaiming issues that make it difficult, if not impossible, to find a valid and economical use case for the technology in any area where it has a competitor. The low conversion efficiency removes any potential for realistic short term or long term energy storage. It manages to surpass lithium ion in a few areas such as high temperatures or high amperage only due to an absolute failure from lithium ion, though it does outperform lithium-ion in unit life and loss over storage time. However, due to the inhibitively low energy conversion efficiency, it is not possible to profit from TES on WPI's scale using current thermal to electric conversion technologies, except when lost heat is repurposed for campus-wide heating. We recommend against possible use of TES on WPI's scale unless heat recycling is considered. If heat recycling is considered, TES is potentially profitable, but the campus infrastructure for heat distribution to buildings must be considered. TES's use cases are limited, but provide a niche market where it is usable and profitable if proper planning and infrastructure for its use are considered appropriate investments.

AUTHORSHIP

This report is the product of the joint collaboration of Muntasir Shahabuddin, Douglas Koethe, Tyler LaCroce and Federico Poggioli throughout six months. The workload was distributed in a way that seemed balanced to the group members. This work was done under the supervision of professor Adam C. Powell, PhD.

Throughout the project Shahabuddin took the leading role of the group by coordinating the group meetings and keeping contact between the different members. A chemical engineering major, his work was mainly focused on writing the methodology, helping with the design of the TESU and with the modeling of the device heat loss to the atmosphere. He also conducted most of the analysis on WPI energy data and RTEP schemes.

Koethe took the initiative early in the report writing process by working on the background and literature review. Later on, he collaborated with LaCroce on gathering information on the electricity market. He also worked on the investment costs and pricing data for materials. A mechanical engineering major, he placed particular effort in gathering information on insulation materials as well as in the market analysis.

LaCroce, an electrical engineering student with interest in power systems engineering took particular interest in gathering information on lithium-ion energy data and in providing accurate metrics to compare its performance to thermal technologies. He provided his greatest contribution in the methodology and findings section, particularly in everything related to the electricity market and the underlying theory of the project.

Poggioli's work during the first part of the project was mainly focused on gathering information from scientific journals for the background and literature review. He also took a leading role in organizing the references, and in reading throughout the paper to ensure there was coherence. A physics major, he later decided to focus his efforts in building the computer model of the TESU device and making sure it was accurate.

TABLE OF CONTENTS

LIST OF FIGURES

LIST OF TABLES

1. INTRODUCTION

As the world comes to rely more heavily on renewables, challenges unique to those energy sources arise. After more than a century of constant rate non-renewable power supply, where electricity production rate is only limited by the amount of fuel combusted, the move towards intermittent wind and solar energy leaves many doubts on its ability to bear the weight of humanity's continuous electrical energy usage.

The main issue in providing consistent energy via solar photovoltaics and wind turbines is that they are inherently intermittent: photovoltaics only produce electricity in favorable weather conditions, and wind turbines only generate electricity in the presence of their namesake. In the short term, unpredictable events - such as a cloud passing over a solar farm - can have significant effects on energy supply in real time. Furthermore, the rise of the temperature of the atmosphere across the globe in the following years is also expected to bring less predictable weather patterns, which could jeopardize an electricity market based on wind, solar, and hydroelectric power sources. The development of market strategies that can effectively be used to incentivize demand stabilization with the intermittent supply of wind and solar electricity, such as Real-Time Electricity Pricing (RTEP), are still in their infancy, and therefore it is necessary to research technologies which can be used for immediate response to energy demand and ensure the supply of electricity always meets energy demand.

Technologies that enable the efficient storage of energy could present a solution to this problem. These would ideally allow the excess electricity from renewable sources such as photovoltaics at their peak production hours to be used to provide energy during periods of high demand. Currently, energy storage technology revolves around electrochemical batteries with varying compositions. Among the most widely used are lead-acid, sodium-sulfur, and lithium-ion [47]. The former two are used in limited scenarios, mostly due to their production cost. However, they both have specific energy capacities low for large-scale energy storage, bearing energy capacities of 30 Wh/kg and 50 Wh/kg respectively, as well as chemistries which are sensitive to volatile weather conditions. Lithium-ion, the current leading energy storage mechanism, can have a specific energy between 60Wh/kg and 150 Wh/kg in its most optimal conditions [5]. While current Lithium-ion specific energy capacities are competitive enough to store energy effectively, they are cost-prohibitive, at around \$209/kWh as of 2018 [6]. If non-renewables are able to offload power from renewable sources 5% of the time, storage prices as high as \$150/kWh will be sustainable. For a system completely reliable on solar PV and wind turbines, costs will have to drop to about \$20/kWh in order to compete with nuclear power plants' production rates [7]. Although Lithium-ion batteries are poised to reach costs below \$150/kWh via economies of scale, its high costs will likely deter its use as the main energy storage medium in order to reach the United Nations' climate goals of 2050.

Thermal Energy Storage (TES), rather than electrochemical energy storage, has been proposed as a potential cost-reduced energy storage method. The concept is quite simple: energy is stored in a thermal energy storage medium (TESM) which is heated using excess electricity to a high temperature, which could be provided by solar and wind power sources during their peak production hours, and thus periods of low real-time price. The TESM is stored in a well insulated container in order to minimize energy loss to the environment. The thermal energy could be then converted back into electricity by using it to heat and evaporate a fluid, which would propel a turbine and generate electricity that could be fed directly into the grid, just as is done in traditional nuclear and coal/gas power plants.

The most common TES implementations are latent and sensible heat storage. Latent heat storage relates to the heat required to change the phase of a material. Compounds capable of containing large amounts of heat during transition are said to have a high heat of fusion, and are known as phase change materials (PCMs). In this publication, the terms TESM and PCM will be used interchangeably while discussing the latent heat storage devices. In contrast, sensible heat storage is just concerned with having heat preserved in a material with a high heat capacity, without changing its state. Both methods can also be combined in varying degrees. Other thermal energy storage technologies involve thermochemical energy storage and cold energy storage. In general, in order for a TESM to be able to store enough heat to evaporate a liquid such as water, it must have a high heat of fusion, a high specific heat capacity, and have a functioning temperature above the boiling point of the fluid.

One of the advantages of TES is that many heat storage media and materials used for its implementation are less expensive than the ones used currently for the most common type of electrochemical energy storage, the lithium-ion battery. Sensible Heat Storage is the cheapest form of TES, ranging from \$0.1/kWh to \$1/kWh [1]. TES is not known for being energy dense, and TES facilities can occupy a great amount of space. This however also depends on the TESM being used. From these statements it is possible to see that TES is a technology with great potential for providing cheap energy storage.

A great number of materials have been studied for TES applications. Previously tested media involve sugar alcohols, ionic salts, and metalloids. Sugar alcohols, such as erythritol, have high heats of fusion, but low melting points and operating temperatures. Though this makes them significantly safer, it also limits the steam turbine efficiency and thus energy output. Silicon, a metalloid, has also been utilized by two companies in Australia as a TESM. It has a significantly higher melting point, allowing for greater steam turbine efficiency. Its radiative emissions at its melting point have also led to considerations of using photovoltaics to recover energy efficiently while limiting maintenance for moving parts [54]. The most discussed potential TESMs are ionic salts. Potassium nitrate, lithium fluoride, and calcium fluoride have all been tested as potential TESMs due to their high heat of fusion and high melting point -- also leading to greater turbine efficiency [9].

While there has been significant research in TESM materials testing and international industrial use as seen in Australian 1414°C’s and Norwegian Energynest’s thermal concrete, use of TES in both utility and private scales has yet to break through, particularly in American markets. Although TES and other forms of energy storage are predicted to be necessary in the ever greener energy market, research into market viability remains limited, including on the local scale.

The objective of this investigation is to evaluate the possibility of implementing a Thermal Energy Storage Unit (TESU) in order to satisfy the energy needs of a small population. For this we use Worcester Polytechnic Institute (WPI), an engineering university in the New England area as a case study. WPI has a population of 6600 students including over 30 buildings that heavily utilize energy consumption for its faculties. There are over 2400 students who live on campus and make use of WPI's facilities all day, including high-speed data network services. and there are three different dining halls to accommodate them. Additionally, research buildings use energy at all times of the day to support certain research projects. As such, WPI could benefit heavily from an energy storage unit to reduce energy costs. A meta-analysis is conducted in order to evaluate possible heat transfer mechanisms, energy conversion methods, and insulation technologies in order to design an optimal thermal energy storage unit for this purpose.

As a result, this project is split into two sections. First, an analysis of possible materials to be used in thermal energy storage units, including insulation and phase change materials, will be combined into a model to calculate relevant parameters for thermal energy storage units. Second, a market analysis of our modeled thermal energy storage unit will be compared against the current leading energy storage technology, lithium-ion.

The current lithium-ion technology and our modeled thermal battery will be analyzed in terms of investment cost and potential profit when used for peak shaving in two different pricing models. These pricing models will be used in tandem with WPI electricity consumption data to determine potential savings for WPI if each type of energy storage is considered. This is done using information from the Worcester electricity provider's pricing data (National Grid). Furthermore, we also evaluate the profits and efficiency of these models if hypothetical case WPI was to participate in a Real Time Electricity Pricing (RTEP) Program, an innovative alternative to fixed pricing schemes with potential of being implemented in order to reduce electricity costs using data from the New England Independent System Operator (NE ISO) [33].

2. BACKGROUND AND LITERATURE REVIEW

2.1 History

Thermal Energy Storage (TES) encompasses a wide array of techniques used to transfer and store heat energy. The efficient implementation of TES systems has been in the interest of humanity since ancient times, beginning with the salesmen of ancient Persia, who transported pieces of ice and sold them in order to help people refresh in the arid climate. Before the advent of refrigeration, ice was used to preserve food by keeping it in a cold enclosed space. It was harvested in cool areas such as lakes, mountains, and rivers to then be transported to ice houses, where it would be buried and covered with sawdust in order to prevent it from melting [8].

The idea of using naturally occurring thermal reservoirs for industrial and domestic applications started in the twentieth century [8]. The first ground-source heat pump was installed in the house of Robert C. Webber in Indianapolis, Indiana on October 1st, 1945. It was a 2.2kW compressor that was hooked to a direct expansion ground coil system in trenches that supplied heat to his house. The modern system of ground water storage, known as Aquifer Thermal Energy Storage, was created in China in the 1960s with the purpose of preventing the land subsidence due to groundwater being extracted for industrial cooling. To help fix this, cold water from the surface was injected into aquifers, which remained cool for long enough to use for industrial applications.

The idea of using TES systems as an efficient method of storing energy for long-term usage was pursued with interest during the oil crisis in the seventies by Scandinavian countries [15]. The initial goal of this endeavor was to store solar heat during the summer for use in space heating over the winter on a large scale, reducing the dependence on oil power plants for domestic heating. Since then, the need for “Green Energy Sources” for the twenty first century catalyzed by the fear of the possible effects of climate change has led to a relatively recent increase of the scientific community on the subject. Until now research has been mainly focused on the evaluation of Phase-Changing Materials (PCMs) for use on Concentrated Solar Power (CSP) Plants, which depend upon appropriate TES systems for their functioning [23]. Furthermore, a significant number of companies providing TES solutions for industry and households have appeared in recent years in North America and Europe. Companies such as Ice Energy (2003), EnergyNest (2011), Viking Cold Solutions (2011), Axiom Exergy (2014) and Neothermal Energy Storage (2015) provide equipment and technology to help consumers reduce the cost of their utility bills and improve energy efficiency.

2.2. Importance

The rise in temperature of the atmosphere due to the combustion of fossil fuels and the ever-growing demand for global electricity provides a solid motivation for research in TES, as it has been considered as a cost-effective alternative to current electrochemical batteries. Electricity markets require the synchronization between hundreds of power plants present in a country in order to ensure a constant power supply. Today's renewable power sources, although effective, cannot be relied upon for the production of the bulk of electric energy. These technologies are weather-dependent, and do not have the property of "inertia", as opposed to a traditional combustion generator. Inertia refers to the ability of a power plant to keep producing electricity for a considerable amount of time after fuel supply has stopped due to mechanical energy still present on the turbine [17]. This is a property useful for coordinating the power production between different plants and ensuring that there are no sudden "jumps" in electric power supply when a generator turns off. TES can be implemented to help renewable energy become reliable sources by solving these two problems by using it to store surplus energy produced during periods of favorable weather, which could be used later to help meet energy supply once the power plant stops producing electricity.

A 2013 report by the United States Department of Energy stressed the importance of energy storage capabilities that can be used independently of renewable power sources for grid stability during electricity blackouts [18]. The report also mentioned that the energy storage capability was only 24.6GW, which was about 2.3% of the total energy production of the country. 95% of these storage solutions consist of pumped water storage, while TES technologies were only around 3%. However, the document does acknowledge some of the advantages of thermal energy storage technologies:

"...The promise of thermochemical storage is the tremendous energy density that it can achieve over most other storage types, ranging from 5 to 20 times greater than conventional storage. Due to its relatively high energy density potential, a significant research and development effort is currently being focused on this type of thermal energy storage, though deployments are limited."

Additionally, TES can also be used on a smaller scale to meet the specific needs of households, buildings and industrial plants. It can also be used to help preserve old historical buildings, as mentioned by Bernardi [16]. Bernardi shows how PCMs are used to maintain the correct microclimate that allows the preservation of artworks inside the building. First PCMs are incorporated in gypsum panels in contact with a wooden panel to test their thermal behavior on the wooden panels under thermal cycles in climate chambers. Additionally, PCMs with silicon coatings in direct contact with a painting were tested in the same conditions. It was found that PCMs are effective at maintaining a climate appropriate for preserving works of art, but can cause damage to the art when in direct contact with it.

2.3. Current implementations of TES

Thermal Energy Storage technologies are classified into four main categories: sensible, latent, thermochemical and cold energy storage [1]. Sensible heat storage, which consists of the preservation of a substance with a high heat capacity on an insulating container, is the most familiar implementation. Latent heat storage relies on phase changes of the storage medium to store the thermal energy, particularly on the energy required to change the storage medium's physical state. Thermochemical heat storage uses reversible chemical reactions to produce heat, and is most useful for long-term storage. Finally, cold energy storage focuses on preserving the temperature of a material (usually water) for later use on domestic applications.

Before going into further detail into the discussion of the different types of TES implementation, it is of good use to first have a notion of what materials are best for these applications can be used. A 2003 study by Zalba, Marin, Cabeza and Mehling [3] concisely summarizes the properties of the ideal TESM in Table 1.

Important characteristics of energy storage materials

Thermal properties	Physical properties	Chemical properties	Economic properties
Phase change temperature fitted to application	Low density variation	Stability	Cheap and abundant
		No phase separation	
High change of enthalpy near temperature of use	High density	Compatibility with container materials	
	Small or no undercooling	Non-toxic, non-flammable, non-polluting	
High thermal conductivity in both liquid and solid phases (although not always)			

Table 1. Important characteristics of energy storage materials [3].

2.3.1. Sensible Heat Storage (SHS)

Sensible Heat Storage relies on materials with a high heat capacity, that is, material capable of holding a large amount of energy in a small temperature change. Houses that directly use sunlight in order to heat water for domestic use are an example of sensible TES. This is also one of the most developed technologies: Boreholes, Aquifer and Water Tank TES are forms of sensible heat storage. The amount of heat present on a given container is determined by Equation 1.

$$Q = mC_p \Delta T \tag{1}$$

where Q is the amount of heat stored in Joules, m is the mass of the storage material in kg, c_P is the specific heat of the material in J/(kgK), and ΔT is the temperature change in the TESM before and after charge or discharge, in either K or C. Common inexpensive materials used in sensible heat storage include clay, iron, aluminum and water.

The temperature range for sensible heat technologies is usually much larger than the range of latent heat storage, as its applications revolve around the concept of changing the temperature of the TESM rather than the physical state. Sensible heat is normally not implemented with gases as it would need to be pressurized, which could cause a catastrophic system failure.

2.3.2. Latent Energy Storage (LHS)

Latent TES (LHS) differs from sensible heat storage due to the fact that it utilizes transition in the physical state of the material as the means to store energy. These are referred to in the literature as PCMs. The amount of heat that can be stored is given by the equation.

$$Q = mH_T \quad (2)$$

where H_T is the specific phase change enthalpy in J/kg. Depending on the material, H_T may refer to either H_{vap}, the enthalpy change between a liquid and gas state, or H_{fus}, the enthalpy change between a solid and liquid state. PCM optimal temperature range is usually straddling its melting or boiling point - where it can capitalize on its enthalpy of fusion or vaporization the best. Zalba, Marin, Cabeza and Mehling [3] classifies PCMs according to their composition into organic and inorganic, and further divides each of these sections into single-compound, eutectic and non-eutectic PCM mixture.

Inorganic PCMs consist mostly of hydrated salts and salt solutions. Hydrated salts act as good PCMs due to their high latent heat of fusion per unit volume, appropriate thermal conductivity, and high melting points. Sarbu and Sevacervici [1] also mention the possibility of using metals as inorganic PCMS, although advise against its use due to the metals' low specific heat and enthalpy per unit mass.

The most widely used organic PCMs are paraffins (Alkenes) and non eutectic mixtures of Fatty Acids. Some of the desirable properties of Paraffins are their large temperature range and stability, besides having specific heat capacity values about 75% greater than those of salts (see Table 3). Fatty Acids also have similar advantages compared to inorganic PCMs, such as latent heat of transition and high specific heat capacity. A better understanding of the overall advantages and disadvantages of different PCM types can be obtained by looking at Table 1. In contrast, Table 2 summarizes the properties of an ideal PCM.

	Organics	**Inorganics**
Advantages	No Corrosiveness	Greater phase change enthalpy
	Chemical and thermal stability	
Disadvantages	Low phase change enthalpy	Corrosive
	Low thermal conductivity	Phase Separation
	Inflammability	Lack of thermal stability

Table 2. Comparison between organic and inorganic materials for heat storage. Modified from [3].

Because phase change stores more energy over a relatively small temperature change than sensible heat storage does, and heats of fusion in common TESMs are high, latent TES has a much higher storage density than sensible energy storage. Some materials can be effective at both types of energy storage, but most are effective at only one type of energy storage. Water, for example, is a common example of a material which can be used for both types of thermal energy storage, but that is best used in SHS due to its high heat capacity.

LHS can be implemented in multiple ways, although its most well-known application is in CSPs. A description of the operation of a CSP is given by Medved, Kvakovský and Sklenárová [2]. Such power plants consist of a large array of parabolic mirrors, known as heliostats, which are used to reflect sunlight to the top of the tower (usually about 80 meters high), in which a device known as a receiver is installed. A PCM (usually a hydrated salt) stored on a “cold” tank is pumped to the top of the tower, where it is heated inside the receiver, and then goes down to be stored on a “hot” tank, from which it can be later be used to generate steam by pumping it through a heat exchanger with water and back to the cold tank. The steam is then used to propel a turbine to generate electricity. A more detailed review of such technology can be found in a 2012 publication by Tian and Zhao [4].

Table 3, adapted from Agyenim, et al. [9], shows different examples of PCMs used in Latent TES, and their most relevant characteristic properties. Choosing an appropriate PCM is not a trivial decision. While high heat of fusion and specific heat capacity may be the most important properties of an effective PCM, physical and engineering constraints in material density, toxicity, corrosiveness and melting temperature may create more reasons for choosing a certain PCM over another. A $LiF\text{-}CaF_2$ mixture may present a high heat of fusion and specific heat capacity, but also require a large temperature to undergo phase change, and also a suitable container for such an amount of stored heat. Paraffin waxes, hydrated salts and their mixtures can be produced with different phase change temperature and properties. A PCM such as water may be suitable for TES solutions on warm places due to its low melting temperature, but may not work in places with seasonal sub-zero temperatures, or with severe daily temperature changes. Socio-economic factors may also influence the choice of an appropriate PCM: The molten salts commonly used on Concentrated Solar Power Plants in the Mojave desert or the arabian peninsula may not be the best option for implementing TES solutions for a residential neighborhood in a crowded city. Location, risk of property damage and funding are variables to be considered with the implementation of any TES system.

One of the challenges associated with TES is that the heat storage medium is hard to insulate well, leading to the stored heat escaping. Also, when performing the phase change necessary for latent heat storage, we must avoid vaporizing the PCM or allowing contaminants which may vaporize at the PCM’s temperature. If that happens, the material will expand, potentially causing an explosion.

2.3.3. Thermochemical energy storage (TCS)

Thermochemical energy storage uses thermochemical materials that store and release heat through a reversible endothermic/exothermic process. During the charging process, heat applied to a material A causes its separation into two parts B+C. The two parts are stored separately until the discharge process, where they are mixed at a suitable pressure and temperature, resulting in a release of energy. The only thermal losses from the products B and C are from sensible heat effects, and are minimal. A study done by Kerskes, Mette, Bertsch, Asenbeck, and Druck [17] looks into the possibility of using thermal decomposition of metal oxides for energy storage, and found that the oxygen evolved can be reused for other purposes. Additionally, the oxygen from the atmosphere can be used to reverse the reaction. TCS is the most efficient method TES, but it is also the most expensive, so it has yet to be widely adopted.

Table 4 shows examples of reactions used for Chemical Energy Storage. Similar to the case of PCMs, there is no single "ideal" chemical reaction that can be used for all TES solutions, as different physical, engineering and socio-economic constraints may apply. For more detailed information on the different types of possible reactions, the paper by Pardo et. al. [30] provides a comprehensive review and analysis of the possible implementations.

Reaction		Temperature (°C)	Energy Density (kJ/kg)
Methane steam reforming	$CH_4 + H_2O = CO + 3H_2$	480–1195	6053
Ammonia dissociation	$2NH_3 = N_2 + 3H_2$	400–500	3940
Thermal dehydrogenation of metal hydrides	$MgH_2 = Mg + H_2$	200–500	3079 (heat) 9000 (H_2)
Dehydration of metal hydroxides	$Ca(OH)_2 = CaO + H_2O$	402–572	1415
Catalytic dissociation	$SO_3 = SO_2 + \frac{1}{2}O_2$	520–960	1235

Table 3. Chemical Reactions used for Thermo-chemical Energy Storage [1].

2.3.4. Cold energy storage (CES)

Similar to LHS, Cold energy storage utilizes PCMs that undergo a liquid-to-solid transition between -5 to 15 °C. The focus of CES systems differs from the aforementioned TES methods because it cannot be used for electricity generation. CES systems can be used for both reducing the amount of electricity consumption by making cooling systems more efficient, and also to shift high electricity demand times to off-peak hours. Cheralathan, Verlaj, and Renganarayanan [24] performed a cost analysis on CES that provided evidence on how an industrial refrigeration system integrated with CES could reduce capital and operating costs of when compared to a normal the cost of just having an industrial A/C system, as well as a reduction in size. Viking Cold Solutions, Ice Energy and Axiom Exergy are examples of companies focused on providing services based on CES technology.

TES System	Sensible	Latent	Thermochemical
Capacity (kW/h)	10 - 50	50 - 150	120 - 250
Power (MW)	0.001 - 10.0	0.001 - 1.0	0.01 - 1.0
Efficiency (%)	50 - 90	75 - 90	75 - 100
Storage Period	days - months	hours - months	hours - days
Cost ($/kWh)	0.1 - 1.0	10 - 50	8 - 100

Table 4. Comparison Chart of TES technologies. Based on content presented by Serbu and Sebarchievici [1].

Compound	Melting temp, T_m (°C)	Heat of fusion, λ (kJ kg^{-1})	Specific heat capacity, C_p (kJ kg^{-1} K^{-1})	Thermal conductivity, k (W m^{-1} K^{-1})	Density, ρ (kg m^{-3})
Water-ice	0	335	4.2	2.4 (liquid) 0.6	1000
GR25	23.2–24.1	45.3	1.2 (solid) 1.2 (liquid)	-	-
RT25–RT30	26.6	232.0	1.80 (liquid) 1.41 (solid)	0.18 (liquid) 0.19 (solid)	749 (liquid) 785 (solid)
n-Octadecane	27.7	243.5	2.66 (liquid) 2.14	0.148 (liquid) 0.190 (solid)	785 (liquid) 865 (solid)
$CaCl_2 \cdot 6H_2O$	29.9	187	2.2 (liquid) 1.4 (solid)	0.53 (liquid) 1.09 (solid)	1530 (liquid) 1710 (solid)
Rubitherm RT					
$Na_2SO_4 \cdot 10H_2O$	32, 39	180	2.0 (liquid) 2.0 (solid)	0.15 (liquid) 0.3(solid)	1460 (solid)
Paraffin wax	32–32.1	251	1.92(solid) 3.26(liquid)	0.514 (solid) 0.224 (liquid)	830
Capric acid	32	152.7	-	0.153 (liquid)	878 (liquid) 1004 (solid)
Polyethelene glycol 900 (PEG900)	34	150.5	2.26 (liquid) 2.26 (solid)	0.188 (liquid) 0.188 (solid)	1100 (liquid) 1200 (solid)
Lauric–palmitic acid (69:31) eutectic	35.2	166.3	2.41 (liquid) 1.77 (solid)		
Lauric acid	41–43	211.6	2.27(liquid) 1.76(solid)	1.6	1.76(solid) 0.862 (liquid)
Stearic acid	41–43 (67–69)*	211.6	2.27 (liquid) 1.76 (solid)	1.60 (solid)	862 (liquid) 1007 (solid)
Medicinal paraffin	40–44	146	2.3 (liquid) 2.2 (solid)	2.1 (liquid) 0.5 (solid)	830 (solid)
Paraffin wax	40–53				
P116-Wax	46.7–50	209	2.89 (liquid) 2.89 (solid)	0.277 (liquid) 0.140 (solid)	786 (solid)
Merck P56-58	48.86–58.06	250	2.37 (liquid) 1.84 (solid)	-	-
Commercial paraffin wax	52.1	243.5	-	0.15	809.5 (solid) 771 (liquid)
Myristic acid	52.2	182.6	-	-	-
Paraffin RT60/RT58	55 to 60	214.4–232	0.9	0.2	775 (liquid) 850 (solid)
Palmitic acid	57.8–61.8	185.4		0.162 (liquid)	850 (liquid) 989 (solid)
$Mg(NO_3)_2 \cdot 6H_2O$	89	162.8	-	0.490 (liquid) 0.611 (solid)	1550 (liquid) 1636 (solid)
RT100	99	168	2.4 (liquid) 1.8 (solid)	0.2 (liquid) 0.2 (solid)	770 (liquid) 940 (solid)
$MgCl_2 \cdot 6H_2O$	116.7	168.6	2.61 (liquid) 2.25 (solid)	0.570 (liquid) 0.704 (solid)	1450 (liquid) 1570 (solid)
Erythritol	117.7	339.8	2.61(liquid) 2.25(solid)	0.326 (liquid) 0.733 (solid)	1300 (liquid) 1480 (solid)
$Na/K/NO_3$ (0.5/0.5)	220	100.7	1.35	0.56	1920
$ZnCl_2/KCl$ (0.319/0.681)	235	198	-	0.8	2480
$NaNO_3$	310	172	1.82	0.5	2260
KNO_3	330	266	1.22	0.5	2110
NaOH	318	165	2.08	0.92	2100
KOH	380	149.7	1.47	0.5	2044
$ZnCl_2$	280	75	0.74	0.5	2907
$LiF–CaF_2$ (80.5:19.5) mixture	767	816	1770 (liquid) 1.770 (liquid)	1.70 (liquid) 3.8 (solid)	2390 (liquid) 2390 (solid)

Table 5. Examples of Phase-changing Materials used in Latent Energy Storage [9].

2.3.5. Energy conversion

Several methods exist for converting heat into electricity. Steam turbines are commonly used to convert the heat back into electricity, as they are one of the most efficient methods for doing this in normal gas power plants. Turbines use pressurized steam to do mechanical work on a rotary shaft, which is connected to the rotor of an AC generator. The cooled steam coming out of the turbine converts back into water. One problem with steam turbines is that the blades experience creep due to high temperatures unless they have protective coatings to reduce oxidation. However, they have a very high power to weight ratio, especially when compared to other generators [25].

Heat Engines such as the Stirling engine also propose an alternative for converting heat to mechanical work. A Stirling engine is constructed with two pistons, a flywheel and a sealed chamber. The linear movement of the pistons inside the sealed chamber is translated into rotational motion by the coupling between these and the flywheel. The constant heating of the gas in one portion of the sealed chamber produces an initial expansion of the gas inside it, which forces the pistons to move. The presence of a heat exchanger material inside the chamber allows the temperature of the gas across the chamber to change, and maintain the reciprocating motion of the pistons. Although it is well known that stirling engines have high theoretical efficiencies and do not produce exhaust, these engines do have serious drawbacks, such as high cost of materials and difficult implementation of an effective heat dissipation system that can maintain a suitable temperature difference between the hot and cold sections of the chamber.

Another method to generate electricity is through the use of a thermocouple. Thermocouples are based on the Seebeck effect, which describes the generation of a potential difference between the two surfaces connected with semiconductors due to a change in temperature in one of the plates. Although thermoelectric generators have no moving parts, their efficiency is rather low (less than 20%). A study by Singh, Nirapure, and Mishra determined that bismuth telluride can be used to make thermocouples with higher efficiencies, although not without an increase in production costs and toxicity [26]. The study found that a safer material set that produces similar efficiency in the mid-temperature range is the family of Mg–Mn silicides.

2.4. Current research topics on TES

Recent developments in Thermal Energy Storage are mostly focused towards improving the efficiency of CSP plants by developing new types of PCMs. A clear example is seen in a 2017 article published by Nature magazine discussing the work of a large group of researchers in a "magnetically enhanced photon-transport-based charging approach" of PCM materials in CSP Plants [27].

District heating and cooling is another popular TES technology, with great acceptance in Europe [32]. District heating/cooling is the implementation of a network of pipes over an entire neighborhood from a centralized location, which pumps water through the network at a fixed temperature for domestic use. Such centralized location then can act as a Sensible Heat Storage water tank or as a heat/cold source. Excess heat from factories and conventional power plants is usually used as the centralized heat source. It is intended to save customers money compared to installing multiple AC units, and also reduce the environmental impact of traditional generators. Local distribution of chilled water can be made by using a heat pump connected to an underground water source.

3. METHODOLOGY

As it was briefly stated before, the objective of this project is to analyze a potential implementation of a thermal energy storage device for meeting the energy needs of a small university in central Massachusetts, and evaluate its theoretical performance compared to traditional electrochemical cells Li-ion cells. In detail, we looked for a profitable way in which TES can be used to either reduce the amount of energy consumption, or reduce electricity costs, of Worcester Polytechnic Institute, and compare the results of this implementation with those obtained by an installation using Li-ion. During this investigation we not only considered the current energy scenario, but also discussed the possible effect of variables such as the growth of renewable energy usage, and the application of policies such as Real-Time Electricity Pricing could have on these energy storage implementations.

In order to accomplish this objective we break down such task into several different parts:

1. *Meta-analysis*: Research methods to improve the overall efficiency of current thermal energy storage units by performing a detailed analysis on each aspect of a unit, including:
    a. The thermal energy storage medium (TESM)
    b. Heat exchangers
    c. High-temperature gradient insulation technology
    d. Electrical to thermal, and thermal to electrical energy conversion methods

2. *Simulation*: Utilize a mathematical model of our optimized system to evaluate the performance of such optimized TESU, without neglecting energy losses by dissipation and conversion from one type of energy to another.

3. *Fixed Price Market Analysis*: Perform a study of the current energy storage market, collect price data of the possible materials that are to be used to build the TESU and to evaluate, based on the results of the mathematical model, whether implementing the optimized TESU design is a profitable enterprise in the current electricity market. This section also takes into account actual information on WPI consumption data.

4. *Real-Time Electricity Pricing Market Analysis*: Investigate whether the use of a Real Time electricity pricing scheme will increase the profitability of the proposed TESU device in contrast to Li-ion technologies.

3.1. Analysis of current thermal energy storage units

3.1.1. Thermal energy storage medium (TESM)

Thermal energy storage can be used in a multitude of applications, and depending on the medium, it can be used for different applications. The ultimate goal in optimizing the TESM used, is in determining the material that optimizes both energy density (energy per unit mass) and specific energy (energy per unit cost). A material having both of these aspects will create a storage unit with low initial investment for equipment and materials, high storage capacity, and low real-estate investment.

Prior research methods involve detailed calorimetry, involving high-cost scientific equipment detailing each material's properties including specific heat values, heat of fusion, melting point, and material density [3,8]. Because we do not have access to such equipment, our project will focus on obtaining and tabulating data from multiple sources which have been able to measure such properties. This involved collecting information from scientific journals, industry and engineering research. We compared the methodologies for each source's research in order to understand any discrepancies, and note them. This also allowed us to combine data to ensure confidence in measured values for material properties [3,9].

Combining multiple sources allowed us to detect gaps in the understanding of TESMs (which we may be able to fill with our own testing), determine which methods are the most practical for our model, and also to create a trustworthy list of material properties based on multiple sources for future research use.

After tabulating data, methods, and qualitative properties, we determined which material optimizes our desired properties: stability, high energy density, and low storage cost. This involved graphing tabulated data to visually represent materials properties. Specifically, we graphed material heat of fusion against cost per unit mass to optimize material cost and energy cost, which we used to narrow down to a list of competitive materials, and then graph properties such as thermal conductivity within the competitive set. Discussion of modeling properties is supplemented with secondary properties which may be useful in other contexts.

3.1.2. Heat Exchangers

Heat exchangers can utilize multiple geometries, flow patterns, and configurations. Similar to how we will analyze optimal TESMs, we will use a meta-analytical method for heat exchanger design. Heat exchangers' functions are relatively self explanatory, but their applications can range depending on the TESM and transfer fluid. In our case, our main method of energy conversion involves a steam turbine, meaning heat must be exchanged between liquid water and our given TESM. The goal in this analysis is to compile a list of heat exchanger parameters, geometries, and flow patterns to optimize an exchanger for our purposes.

Similar to our TESM meta-analysis, this involved data-gathering from scientific publications. Traditional heat exchanger property measurement involves the use of isothermal contour plots to optimize geometry, and material temperature time curves to determine heat transfer rate [9]. However, for the purposes of our model, we decided to use a simplified straight-tube heat exchanger to bypass the likely computation-heavy analyses of other, practically better heat exchangers.

We analyzed multiple heat exchanger contexts, types, and variables to determine which was the most optimal for our model. Our heat exchanger design was guided by our energy conversion type as well. For a traditional steam turbine energy conversion method revolves around transferring heat from our TESM to water, while thermoelectric generators require heat transfer to a flat thermoelectric generator unit.

Our weaknesses here were in our time and modeling constraints. Since heat exchanger designs can be made considering a great number of variables, it was difficult to decide on a specific heat exchanger design based on several particular qualitative parameters. The difficulty here was in quantitatively analyzing the best functioning heat exchangers with a dearth of empirical data in the context of our unit. Our decision to model a straight-tube heat exchanger creates an opening for error and improvements in the accuracy of our model, although our modeled heat exchanger follows a worst-case scenario, simplified heat exchanger--improvements in the heat exchanger from a straight-tube model are simple to make and result in significant improvements.

3.1.3. High-temperature gradient insulation technology

Insulation technology is widely used and has a long history--ideal conditions for power plant design, residential living spaces, refrigerators, and many more products search for the ideal insulation--allowing little to no energy transfer across a gradient. Because of its broad usage, meta analysis of insulation technologies involves research into multiple contexts. The objective here is to categorize multiple types of insulating material, optimizing for low thermal conductivity. Research into other insulation parameters and methods supplements the materials study.

Insulation technology revolves around the concept of a material with low thermal conductivity acting as a barrier between items of differing temperatures. Because our model may involve a 100°C to 800°C temperature difference between the inside and outside of the storage unit, high temperature insulation technologies will be researched. Since we worked with high temperatures, there are multiple contexts we researched--namely refractory materials. Because metal processing factories require similarly high temperature gradients, research into similar refractory technologies was instrumental in guiding the design of our insulated TESM container. The main parameter of interest is in material thermal conductivity (W/(m*K)). Functional temperatures were also researched, as they guided which types of TESMs/which melting points were possible. Research on cost and availability of each material using online sources was performed as well.

3.1.4. Energy conversion methods

Energy conversion is a major aspect of our system. Converting into thermal energy from electricity is simple and efficient, and can be done such as electrically by using resistive heating, or placing a heat pump next to a heat exchanger. Resistive heating allows for power draw directly from the grid and convert it to thermal energy with nearly 100% efficiency [30]. Geothermal heat pumps are significantly more efficient for low temperature gradients near atmospheric temperatures, but are not suited for the temperature gradients created by many of the TESMs we will analyze [31].

The conversion of heat to electricity is more complicated. Our thermal to electrical conversion involves another heat exchanger acting as a boiler. This boiler would be filled with water from a storage tank. The boiling water would then be pumped into a turbine to generate electricity. This section offered the most difficulty in creating an efficient model.

There are few ways to determine energy loss in generators. Measuring exactly how much energy is converted by the generator could be done in multiple ways, usually by measuring via some sort of load-- such as using a resistor to simulate load, charging a battery, or powering an LED. Charging a battery presents the issue of both determining the charge of the battery and its loss of efficiency. The LED can present issues of locking the voltage, which, if it is not correct with the output voltage of the motor, can create a large current and become a safety issue. Both of these methods are also susceptible to having far more loss due to the wire used to connect the LED or battery. A large resistor though would make the extra resistance from wire negligible. It also does not pose a risk if the voltage or current is abnormal or higher than expected.

In order to conduct the analysis, however, we must use current parameters for energy conversion in technologies used today. Research into appropriate energy conversion methods was made, and given the scope and technologies of our project, we determined steam turbine generators to be the most appropriate conversion method. Our project is based on the Siemens D-R C steam turbine generator, able to output up to 2500 kW--about 500kW over WPI's peak consumption. Datasheets and information provided by Siemens were used to estimate conversion parameters in our modeling [56]. To estimate efficiency of the turbine, we used Carnot efficiency multiplied by a correction factor to account for non-idealities, as true turbine efficiency was not available to us. Carnot efficiency (η) is defined as:

$$\eta = 1 - \frac{T_c}{T_H} \tag{3}$$

Where T_c represents the temperature of water entering the turbine, and T_H represents the functioning temperature of our TESM/PCM. We used 0.8 as a correction factor given the operating temperature difference of the turbine and our unit. This efficiency represents an idealized efficiency of the system, and thus is an overestimation of true efficiency.

The weakness of this analysis lies in that most of the modeling is based on ideal systems. For example, the generator would be modeled as with a static efficiency based on the theory above, yet this would not be accurate to the variable efficiency the motor can put out over time. Thermodynamically, the modeled system efficiency also is modeled near the highest possible efficiency given the parameters we input. Our correction factor may not account for all of the startup or shutdown loss and other more minute details would not be represented in the overall model. This problem of using theory based modeling resonates throughout the entire project, but should still provide enough information to show if the concepts are possible.

3.2. Economic and market of cost-of-storage against current lithium-ion technologies

The physical limitations of a thermal energy storage unit rely on three major numbers: the cost of storing a unit of energy, the amount of stored energy per volume, and the amount of energy stored within a mass. All of these factors have different levels of importance based on context. For instance, if thermal energy storage was better than lithium storage in cost but was significantly worse in storage per mass, it would not be helpful for energy storage in spacecraft, where minimizing mass is prioritized over cheap long term storage. These factors may scale differently or non-linearly as well, meaning that certain methods may be better or worse on different scales. These three major factors and how they compare to lithium storage were the focus of our research.

The first factor is the cost of storing energy. This number can most easily be compared by examining the efficiency over time. The efficiency over time can be tested by putting in a certain amount of energy to the storage medium and seeing how much can be recovered at different times. The cost of storing energy in the system is then calculated from the values obtained. In the context of thermal energy storage, energy can be lost during three overarching processes. The first is during the conversion of electrical energy input into thermal energy in the storage medium. The second is loss to ambient temperature while the medium stores said energy. The last major source of loss is in converting the stored thermal energy back into electricity. The losses from each of these processes can then be combined to provide an overall energy lost per unit time and thus provide the efficiency over time. This provides a starting maximum efficiency and the rate of which the efficacy decays. The loss of energy per hour would then provide the equation for modeling the efficiency over time. An integral of the loss graph can provide overall loss to calculate average loss in a time frame. This allows systems to be easily tested and compared.

The second factor is storing energy per mass. This comparison provides the most useful data when comparing energy per mass, per hour. This provides the most useful data and can be gathered alongside the experiment for efficacy over time. The data would allow for objective comparison of different mediums of storage when used in different contexts. TESMs and models can be optimized for both short term, low supply methods, as well as long term, high demand-bearing applications. It also provides scalable data, so the amount of storage medium needed could be determined and analyzed under different conditions. However, the method would not reflect the mass or cost of any supporting equipment required, namely storage and insulation. First, the amount of energy between 100 °C and the melting point of the TESM would be calculated. Since the TES only becomes hazardous when the TESM changes into a gas and increases in pressure, the entirety of this difference between 100 °C, the boiling point of water, and the boiling point of the TESM. It follows that the amount of "useful" energy stored in the TESM, which can be converted back into electricity, is the amount of heat stored between these two temperature boundaries. The heat of vaporization, specific heat capacity, and temperature change, multiplied with the mass of the substance provides the starting efficiency of the system. Combine this with the data of energy loss gathered in the first test allows the data to be extrapolated over time. Lithium batteries would have their maximum energy calculated via current methodology, then have their mass and decay compared against those of each TESM.

The third factor is storing energy per volume. Similar to energy per mass, this comparison is most helpful when comparing energy per volume per hour. It provides the most useful data as it can show both short term and long term storage where the most important factor is volume. Most of the data required for this statistic can be gathered in the same experiment as the two prior statistics. The rest of the data can be or has been calculated during the prior statistics. As done previously, the TESM has its maximum energy calculated by determining the difference to change from 100C° to boiling/melting point, or the energy required to induce a phase change, and adding that to the calculated heat of fusion. The calculated maximum energy would then be divided by the volume to provide a starting maximum energy per volume. The rest of the data would then be extrapolated using the heat loss of the TESM in the insulated unit. The lithium battery would follow a similar path as well. The battery would have its maximum energy determined by conventional means. The energy would then be divided by the measured volume and using the measured efficiency rate, a graph over time would be created.

Both energy per unit mass and energy per unit volume carry different values depending on the market and use. In the most extreme examples, aerospace applications for fuel and energy storage require high mass and volume energy density to ensure least-practical-load for the vessel. For large commercial hybrid electric aircraft, the required energy density must remain between 750-1000 Wh/kg [29]. Recent silicon-based thermal energy storage units average nearly half that at about 390 Wh/kg [28].

The difference in the myriad energy markets is best visible in the value of these metrics alongside others. We will perform an analysis of WPI's consumption and local market pricing of electricity to determine how TES performs against lithium-ion on a scale relevant to the campus. By calculating the above parameters of TES, we will be able to understand the economic viability of the technology as a potential competitor to lithium-ion and as a possible source of income for WPI.

Issues revolving around estimating possible economic benefits is that all assumptions in other parts of our modeling will compound and affect the results we calculate. Many of our assumptions may not represent parameters of a practical unit. Because of this, there are many aspects of modeling which will greatly affect the economic analysis, particularly in the assumptions of efficiency and loss. We have done our best to account for such inconsistencies and chosen assumptions which will still result in similar recommendations for each technology, such as by reducing Carnot efficiency by a factor to account for non-reversible process.

3.2.1. Economic Analysis of Different Market Pricing Methods

In order to perform a market analysis, we focused on calculating profits based on local pricing models, the modeled parameters of the thermal battery, and researched lithium-ion parameters. Data analysis follows WPI's consumption data provided by WPI Facilities, as well as real and extrapolated pricing regimes.

Consumption modeling is consistent across both pricing models since it follows WPI's consumption. In order to model consumption accurately, we chose to analyze four months of the year, each representing consumption during the respective seasons. We determined January, April, July, and October were appropriate months to represent winter, spring, summer, and fall respectively. Consumption data values from each day for a given month were combined and averaged to create an "average day" for that month in terms of consumption. During peak and off peak optimized charging times (determined based on the pricing model), the integral of the power consumption over that period of time was calculated using the trapezoidal rule method in Python. The integral of power consumption over a period of time provided us with energy consumption over the set period of time and dictated calculations for profits and savings by determining current costs for energy consumption by the university.

Pricing data differs across the US as different parts of the country adopt varying amounts of renewable energy and in response, varying pricing models. Our analysis mainly follows the peak and off-peak pricing of National Grid (Worcester's main electric utility). Analyzing pricing using the peak and off-peak pricing model is significantly simpler than analyzing true real time pricing, as price is simply treated as a scalar which changes at set times provided by National Grid.

Although not completely accurate to the consumer level (as we used wholesale real time market pricing), we also determined analyzing a true real-time pricing model would be appropriate to understand the possible use-cases for different storage technologies. To estimate this, we used wholesale energy pricing from the New England Independent System Operator (NE-ISO). The ISO provides its data online, although the pricing does not reflect consumer-level costs. In order to analyze the real-time pricing, we simulated an "average day" in four representative months: January, April, July, and October, each representing winter, spring, summer and fall respectively. Averaging out pricing values for each day for particular months provided a representative "average day" in terms of pricing for each season, similar to the "average day" of WPI's consumption in each season. Using this "average day" model, we determined peak and trough costs of each average day in the four seasons. The average day pricing was then used in tandem with the consumption modeling average day. The trough and peak prices are used to calculate a ratio between each, which will be used to represent minimum efficiency of systems under real time pricing.

3.3. Use of a model of optimized system to obtain data to supplement economic and engineering analyses of thermal energy storage units

Acting as a culmination of all the individual setups, a model will be generated to simulate the entire TESU. The objective of this model is to show if it is remotely possible for the structure to exist and be economically viable when combined with real time energy data.

We will build the model using the individual modeled idealistic components. From the model we will work to optimize and find the most cost effective viable parts to maximise the potential economic advantage. The TESM, heat exchanger, insulation, and energy conversion efficiency will all be variables that can be adjusted and be changed based on the material they are representing. If there is economic plausibility, then a number of cost models with payback times will be generated alongside the efficiency ratings.

This scale model data will also be used to compare to lithium-ion data to determine if lithium ion energy storage technology is more or less viable than the proposed thermal device. This will be done by applying the same test to lithium ion as to the thermal storage unit to be able to directly compare them in different areas of functionality.

3.3.1. Heat Loss From Modeled System

A possible downside to TES is in the constant energy loss to the significantly cooler surroundings. In order to determine thermal energy storage's effectiveness for use at WPI and in the market, accounting for its energy loss to the atmosphere is instrumental--particularly in determining profit losses relative to the longer-term storage found in lithium-ion.

In order to determine heat loss of the unit under different conditions, initial conditions for storage were determined using the unit Mathematica model, under the assumption of 1 MWh of effective storage for the unit and comparable lithium-ion units. This assumption was used to model a cylindrical salt storage tank for determination of tank inner surface area in contact with the salt. To calculate the heat loss, we determined to split the problem into multiple heat transfer problems across different interfaces, as seen on Figure 1.

The heat transfer problems were split into three different sections around each interface: the TESM PCM to the tank wall, the insulation walls, and the outer tank wall to the atmosphere.

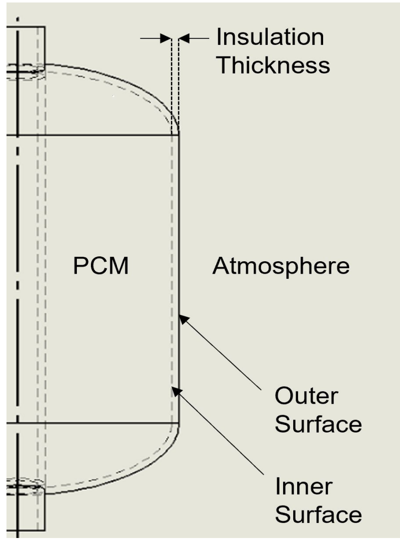

Figure 1. TESU Insulation Diagram

Depending on the interface interactions, an overarching heat transfer equation was developed with the goal of iterating through insulation thicknesses to calculate percent heat loss per hour from the TESM container. The general equation for convective heat transfer is:

$$q = h\Delta T \tag{4}$$

Where h is the coefficient of convection, and ΔT is the temperature difference between the material at the interface and the adjacent fluid. Based on the previous diagram, the types of heat transfer were determined based on material interactions. Inside the tank, the TESM is a liquid, allowing us to assume convective heat transfer. Inside the wall heat transfer is done via conductive heat transfer due to its solid nature. The gaseous atmosphere also acts as a fluid creating convective heat transfer at the outer surface. We then solved each interface equation and combined them to result in a large equation returning heat flux out of the TESM storage tank as a function of insulation thickness and a multitude of parameters depending on material properties. The overall equation is simplified as follows:

$$q = \frac{\Delta T}{\frac{1}{h_{TESM}} + \frac{\delta}{k_{ins}} + \frac{1}{h_{air}}} \tag{5}$$

Where δ represents insulation thickness and k_{ins} represents insulation thermal conductivity. To calculate the heat transfer coefficients of the TESM 'h_{TESM}' and air 'h_{air}', we used the following equation:

$$h = \frac{Nu\,K}{L} \tag{6}$$

Where Nu is Nusselt number of a material and L is the length of the surface interface, which is specific to both material properties and surface interactions for heat transfer. Our TESM tank is a cylinder. Because the liquid salt viscosity is so high, convection flow is low, and thus the Reynold's number is low. Because of this, we can treat the cylinder as a vertical wall for the purposes of heat transfer to the atmosphere. The Nusselt number is represented by:

$$Nu = 0.59Ra^{1/4} \tag{7}$$

Where Ra is the Rayleigh number, specific to material properties:

$$Ra = \frac{L^3 \beta g \Delta T}{\nu^2} \tag{8}$$

Where L is length of the surface interacted with (in this case, the height of the cylindrical tank), β is the material's thermal expansion coefficient, g is gravity, ΔT is the temperature difference between the TESM and air, and v is kinematic viscosity [57]. We assumed the viscosity of material within 50 degrees of their melting points, or in the case of air, at room temperature. The same process was used to calculate the overall heat transfer coefficient of air as well.

The heat transfer coefficients as well as the insulation thermal conductivity were combined in the above heat flux equation. In order to determine total heat flow out of the system, the following equation was used to normalize heat flux into total energy flow using container surface area:

$$Q = qA \tag{9}$$

Where A represents container inner surface area, t is the time and Q represents total heat flow in units of power. After determining total energy flow rate out, conversions were used to calculate energy loss per hour relative to the battery's energy capacity using total battery capacity and heat flow out of the battery:

$$Percentage\ of\ energy\ lost\ per\ hour = \frac{3600Q}{Total\ battery\ capacity} * 100\% \tag{10}$$

4. FINDINGS

4.1. Theoretical investigation of possible Thermal Energy storage solutions and modelling of a Thermal Energy Storage Unit (TESU)

4.1.1. Thermal Energy Storage Device Operation Procedure

The proposed thermal energy storage device functions following the outlined steps:

1. Electric energy is dissipated by a resistor present inside a PCM tank that is custom built in order to allow efficient dissipation of energy from the resistor to the PCM material, as well as to the water source that is intended to carry out the work of converting the stored thermal energy back into electrical energy via the Rankine cycle. During this stage, the PCM is only storing energy, and therefore we refer to the device as being in *charge mode*. Ideally, the device is set to be charging during low-peak hours right before the start of the peak surge in demand. Since the material being used is a phase changing material, the TES device is considered to be charged when all of the material has undergone a phase transition.

2. Once the device is charged and demand is about to increase, water is pumped from an external reservoir to the PCM tank and throughout the system. Depending on the turbine and the tank parameters, the water will need to circulate through the piping several times until the difference in temperature at both ends of the PCM tank is high enough to exert the necessary work on the turbine to produce the desired constant power output.

3. After the desired temperature range is reached, the device will operate in what is known as the *discharge mode*. The device is kept running until the total effective energy (latent heat) stored is transferred to both the water and its surroundings.

4. As the amount of effective energy stored in the device reaches its minimum value, the turbine is turned off and the conventional power supply is restored.

4.1.2. PCM Tank Model

A computer program was written in order to accurately simulate the operation of the device. The software Mathematica was chosen due to its simple syntax and ability to handle operations involving a high level of abstraction with ease. The purpose of the program was to accurately calculate the heat flow rate between the PCM and its surroundings, both to the water inside the inner tank pipe and to air in the outer surface of the tank. This calculation of the flow rate was necessary to calculate the power output and the physical dimensions of the device.

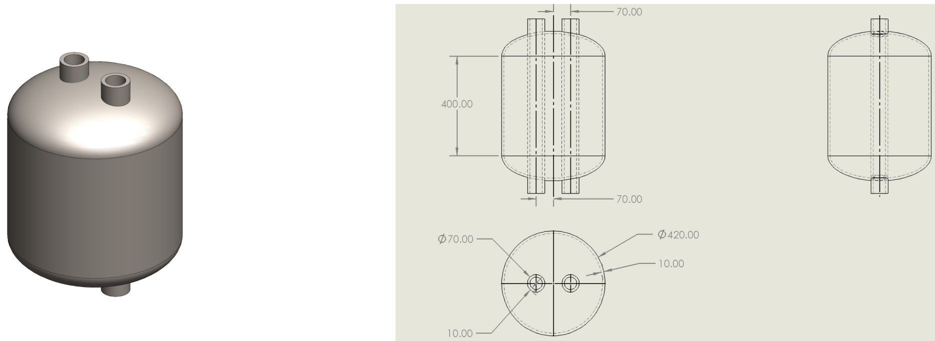

Figure 2. PCM Tank Model Detail. The left pipe is the place where the heating element is to be placed, while the right one is connected to the water pipe and the rest of the components of the system. Dimensions are not to scale.

Figure 2 shows a CAD Model of the modeled PCM tank: A large metal vessel filled with PCM with two longitudinal openings which cross across the inside of the tank. The left opening holds a resistive heating device in place which will heat up the PCM, while the right pipe contains the water that will get heated as it goes through the inside of the tank and flows to the turbine.

The proposed model, although simply a sketch, makes it straightforward to explain the operation of the device, and is simple enough in order to carry out calculations. Accurately modeling this device turned out to be more difficult than we had originally thought. In order to calculate the amount of heat that transfers from the PCM to the water and measure the amount of time taken s to heat up the water present in the pipe it is necessary to break up the problem into several different parts:

1. First the heat of the PCM gets transferred to the inner water pipe during a specified time interval by convection. For modelling purposes we utilize the discrete version of the equation that describes the convective heat flow between two material surfaces:

$$q = -h(\Delta T)^n \tag{11}$$

Where q is the heat flow, h is a constant dependent on the properties of the material (which may vary depending on the temperature of the system), A is the outer surface area of the water pipe, ΔT is the temperature difference between the two boundaries and n is a unitless parameter. The value of n was determined to be 5/4 due to the temperature dependence of the Grashof number.

2. The heat from the pipe is then transferred to the innermost pipe surface by conduction, which is given by Fourier's Law of Heat Conduction:

$$q = -k\Delta T/\Delta x \tag{12}$$

Where k is the thermal conductivity of the pipe surface metal.

3. Finally, the heat transfer to the water occurs during a given amount of time in a way that is not uniform: Since water is assumed to be constantly flowing through the pipe at fixed temperature and pressure conditions, the speed at which the water flows must be taken into account in the calculation in order to make sure these parameters are met in order to ensure turbine produces a constant power output. The mass-energy balance of the section of the PCM tank is given by the equation below. The meaning of the variables of the equation is seen in Figure 3.

$$q_1 + q_2 = q_3 \tag{13}$$

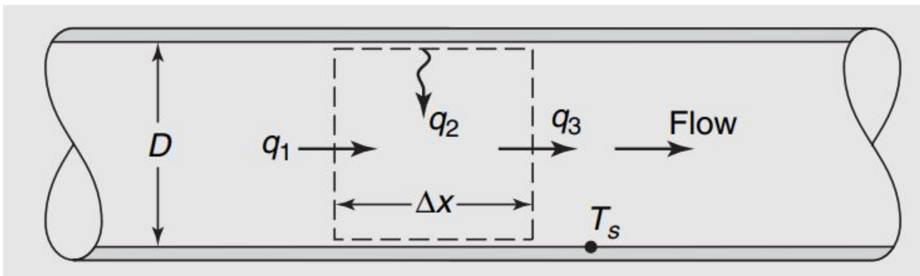

Figure 3. Inner Water Pipe Heat Flow Sketch and governing equation. Taken from [52].

From this energy balance follows that the temperature of the inner fluid in the pipe can be calculated by using the equation, taken from [52]:

$$ln((T_L-T_S)/(T_0-T_S)) +4Lh/(D\rho v_x c_p) = 0 \tag{14}$$

Where T_L is the final fluid Ts represents the pipe surface temperature, T_0 is the initial fluid temperature, ρ is the density, v_x the velocity, *c* the specific heat capacity. h is the convective heat transfer coefficient while and *L* and *D* correspond to pipe length and diameter, respectively.

Setting the heat flux equations of the PCM to the pipe and from the pipe to the water equal to each other allows us to obtain a single equation that can be used to solve for the total value of q_2 for a small section of the pipe. An iteration loop is then implemented in order to carry this calculation along the different segments of the pipe. Another iteration loop across discrete time values is also implemented in order to simulate the changing values of the temperature of the water as the heat gets distributed through the system. These iterations are necessary in order to adjust the program in order to accurately model the change in the materials properties. While some parameters of the flux equations remain constant throughout charge and discharge mode, several of these are temperature dependent, and can vary greatly if the material undergoes a phase change (such as the density of the water, for example).

As in any thermodynamic cycle, it is necessary to properly account for non-reversible changes in the system by considering the presence of an upper limit to thermodynamic efficiency and also heat loss due to propagation to the air immediately outside the tank. The heat transferred to the air is assumed to be dissipated instantaneously in order to keep the temperature of the air constant. This contrasts with the calculation of the total heat transferred to the steam, which does assume this is flowing through the pipe at a constant velocity. As mentioned before, In order to ensure consistency with the second law of thermodynamics, we assumed the efficiency of our cycle was 40%, which is below the Carnot Efficiency for an engine working between hot and cold reservoirs at 334 and 25 ºC, respectively (51%).

From the results obtained we believe that in order to produce 1MW of power output for 1 hour it is necessary to use about 33,835 kg of KNO_3. This is assuming the device only operates using the amount of heat stored as latent heat, and has a temperature drop of about 50 K in the turbine. The results of the simulation can be seen on Figure 4, which shows the initial and final water temperature distributions of the water as the device is put into charging mode and the water starts to heat up. Results from the model show that during 60 minutes as the water heats up from 373 K (100 ºC, boiling temperature of water) to 607 K. (334 ºC, the PCM phase transition temperature) The change of the properties of water as temperature increases and the decrease in temperature difference between the PCM and steam explains the observed nonlinearity of the graph.

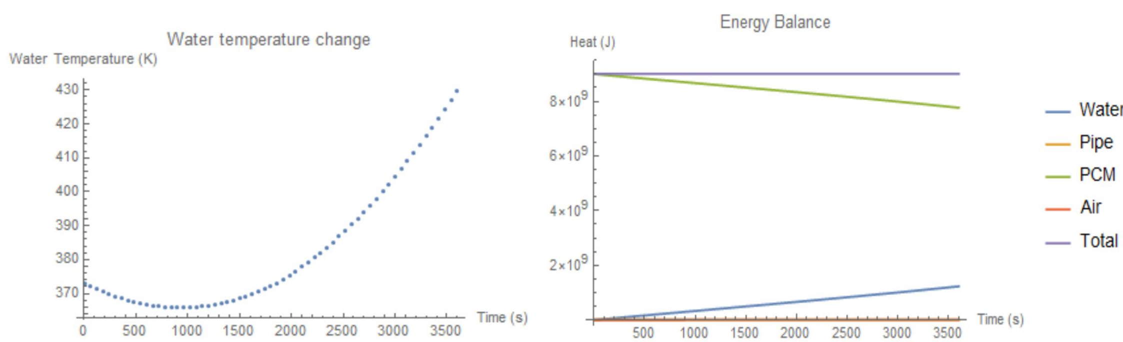

Figure 4. Water temperature and Energy balance graphs. (See note on Appendix A).

The amount of heat stored in the PCM tank at the beginning of the discharge cycle is 2.5 MWh (9.0 GJ). On the Energy balance graph, the purple line represents the total energy of the system, while the green one refers to the amount of latent heat stored in the PCM Tank. The blue, yellow and red lines correspond to the heat being transferred to the water, air and the metal surface of the tank itself, respectively.

Figure 4 also shows the energy balance of the system as heat is dissipated across the system in order to show the consistency of our model, from which the power output and time at which the latent energy stored in the tank will be depleted were calculated. The energy balance graph shows how the total energy of the TESU and its immediate surroundings in purple, while the green one refers to the amount of latent heat stored in the PCM Tank. The blue, yellow and red lines correspond to the heat being transferred to the water, metal and the air outside of the tank itself, respectively. As expected, heat stored in the PCM tank decreases as it is transferred to both the metal container, the water and to the air. As it is desired, most of the heat gets directly dissipated to the water, however, a significant fraction also gets dissipated into the air as well, which gives importance to the use of effective insulation materials in order to reduce this.

4.1.3. Heat/Energy Loss to Atmosphere

The main drawback of using thermal energy storage over traditional electrochemical storage is in its constant energy loss due to high temperature storage. The higher the temperature TESM, the faster energy will dissipate from the storage unit. As part of developing a holistic understanding of TES's possible roles for storage, determining the energy loss to the atmosphere is an integral part of our model.

Given our analysis of appropriate PCMs for use in thermal energy storage, KNO_3, or potassium nitrate, was our final decision and heavily affects energy loss calculations. Under the conditions of using KNO_3 as our TESM, and in a cylinder with a diameter of 1.65m and height 7.50m, insulation correlates to energy loss per hour in the following graph:

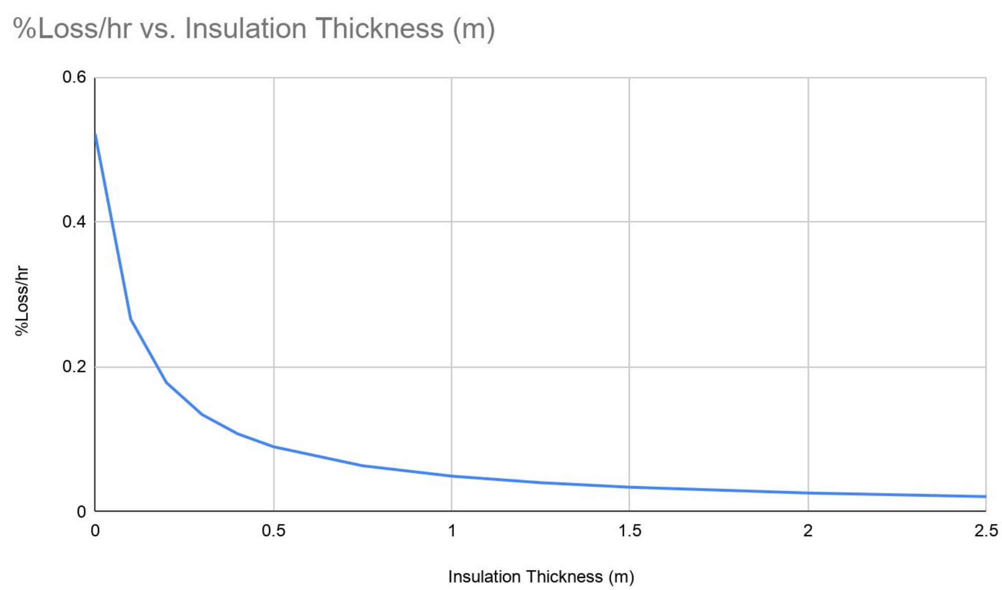

Figure 5. Percentage of heat loss per hour versus insulation thickness

Insulation thickness has diminishing returns at larger thicknesses, as is expected of the inverse relationship with insulation thickness. To limit insulation usage to a reasonable amount while ensuring reasonable heat loss per hour, our modeled unit has 1 meter of insulation, correlating to about .049%/hr of loss to the atmosphere. This insulation modeling accentuates one of the core limitations of thermal energy storage--its demand for real estate over lithium-ion. Although we compare salt energy densities and may think of them as the sole contributors to energy density of the system, large volumes of insulation lower the overall unit energy density considerably.

The unit, although only effectively storing about 1 MWh, will require a moderate amount of insulation -- and space to house the unit -- in order to function following this model. If the percentage of loss per hour is more lenient, the decay in insulation thickness required is quite drastic, so in short term storage conditions, less insulation can lower space and investment cost while maintaining utility. We will assume a 0.047% loss for the rest of this project, although loss can be adjusted for appropriate settings where storage time must be longer. Because our project requires only about a 3-5 hour storage period, as will be detailed below, this loss is reasonable for this context, and is flexible enough for longer storage projects. As is apparent against turbine efficiency, loss to the atmosphere is not currently the limiting factor in profiting from TES.

4.2. Theoretical investigation of possible electrochemical energy storage solutions and investigation of current Lithium-Ion storage technology

One of the biggest threats to the viability of a product is in its competitors. The main competitor to TESU technologies are large lithium-ion batteries, currently the most popular energy storage technology. Lithium-ion is considered better than the lead acid batteries because it has a starting 99% charge efficiency opposed to lead acid's 90%. One of the main drawbacks is its large initial depletion rate. Lithium-ion loses 10% of its total charge within 24 hours of charging and continues to lose charge exponentially [40]. This is one aspect we expect TES technologies to have a greater advantage.

An issue with long term energy storage in lithium-ion batteries is the high depth of discharge. Depth of discharge is the percentage of the battery which should not be discharged to protect the integrity of the battery [40]. Every cycle of discharge causes some damage to the battery. On average the battery has a depth of discharge of 30% and a total cycle life of 1000 cycles [40]. These cycles also are significantly lowered by discharging at a higher amperage, for instance a small battery cell can reasonably cycle around 10,000 times with a discharge rate of 2A, but when the amperage is increased to 20, the cycle rate goes down to 500 cycles. Most homes operate with 15A and 20A breakers, so pulling this high of an amperage is not realistic. This makes a lithium ion a good choice for small amperage structures such as home solar or cell phones. Power supply stations operate around 200A per generator. Technically multiple cells can be arranged in a combination of series and parallel connections to create a battery able to handle these high amperages, requiring expensive battery management systems to avoid cascading failures from voltage differences between cells. The use of TES technologies may complement lithium-ion in that they perform better in larger scales, while lithium-ion requires further monitoring technologies at larger scales. TES does not require the large-scale battery management systems that lithium-ion does, further decreasing its cost relative to lithium-ion. .

Another major issue lithium has to do is with the operational temperature range. Lithium batteries begin to fail at temperatures of 30° Celsius and above [40]. Although it is still possible to operate these kinds of batteries on this range, there would be a large decrease in efficiency. This is also a point in favor of TES technologies.

A thermal energy storage system compares well to lithium-ion storage in very few, but important areas. In both high current and high heat, lithium-ion experiences near complete failure [55]. Thermal energy storage holds up in both of these situations, as energy output is only limited by turbine parameters, and high temperature climates would only serve to benefit thermal energy storage. In the example of a very large generator outproducing the load of the grid, it could be more profitable to begin to charge a thermal battery than to slow down the generator. Another case could be very deep drilling, because it could serve as reliable power storage if the temperature gets very high.

4.3. Market Analysis for proposed thermal and lithium-ion energy storage solutions

4.3.1. Introduction

This section presents comparisons between thermal energy storage (TES) as well as lithium-ion battery storage technologies. Market analysis is split into two sections: A performance of the TES unit for WPI's use, and a performance comparison to lithium-ion with the current electricity market and the real-time electricity pricing model.

4.3.2. Energy Storage Investment Costs

Currently, Lithium-ion battery storage is the most efficient and ubiquitous storage technology. As of 2018, prices for lithium-ion battery storage have plummeted 85% since 2010, and are projected to lower even more in the future (Figure 6).

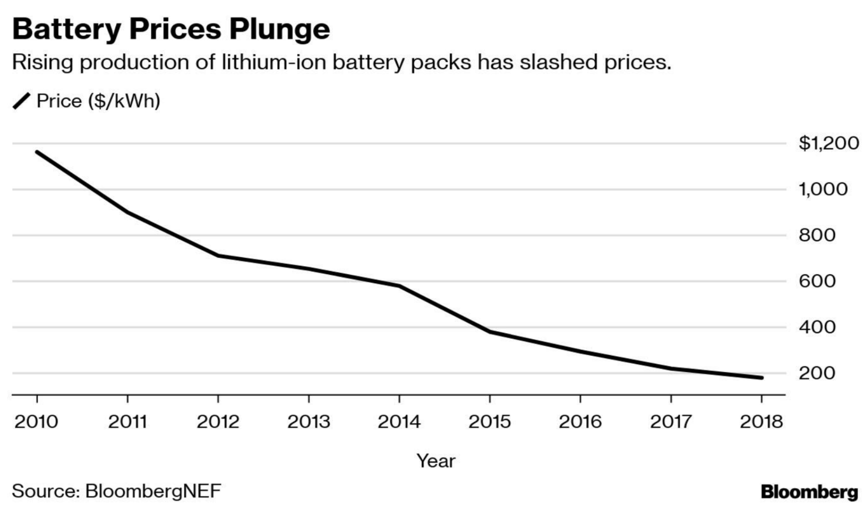

Figure 6. Lithium-ion Pricing by Year [48].

However, the still-high cost of lithium-ion and limited availability may lead to damper on these expectations [34]. For example, in order for the world to reach 100% EV penetration, (100% dependence on electric vehicles for transportation), there needs to be an increase of

2898% in the amount of lithium currently used in the automotive industry, which may be improbable, or at the very least, may come with a large environmental cost.

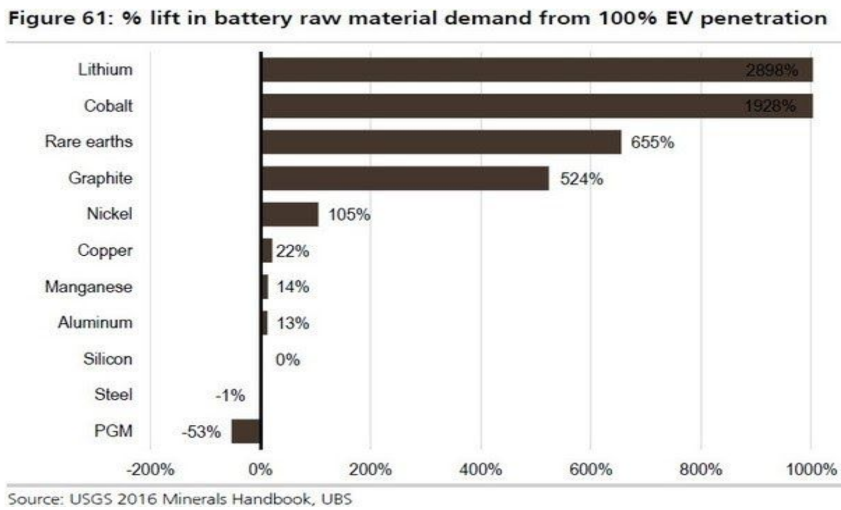

Figure 7. Required Increase in raw material demand for 100% EV penetration [50].

To reach 100% dependence on renewables, storage prices are recommended to drop to about \$20/kWh. If 5% of demand is handled by non-renewables, storage cost can drop to \$150/kWh [36]. Although the latter goal is within reach, 100% dependence on renewable energy requires storage costs that are currently far out of reach for lithium-ion. Right now, long term energy storage with lithium-ion is still prohibitively expensive. As such, it is likely that other avenues of energy storage such as TES will become more appealing.

4.3.3. TESM and Insulation Analysis

4.3.3.1. TESM Analysis

Benefits of thermal energy storage design revolve around cost effectiveness. Determination of the thermal energy storage medium (TESM) is paramount for unit cost, capacity, and volume. Cheap materials ensure lower investment costs, while materials with higher heat of fusion allow for more latent energy storage per unit mass. Two of the most important factors to look at are the price of insulation material, and the price of a TESM. These can be observed on Figure 8.

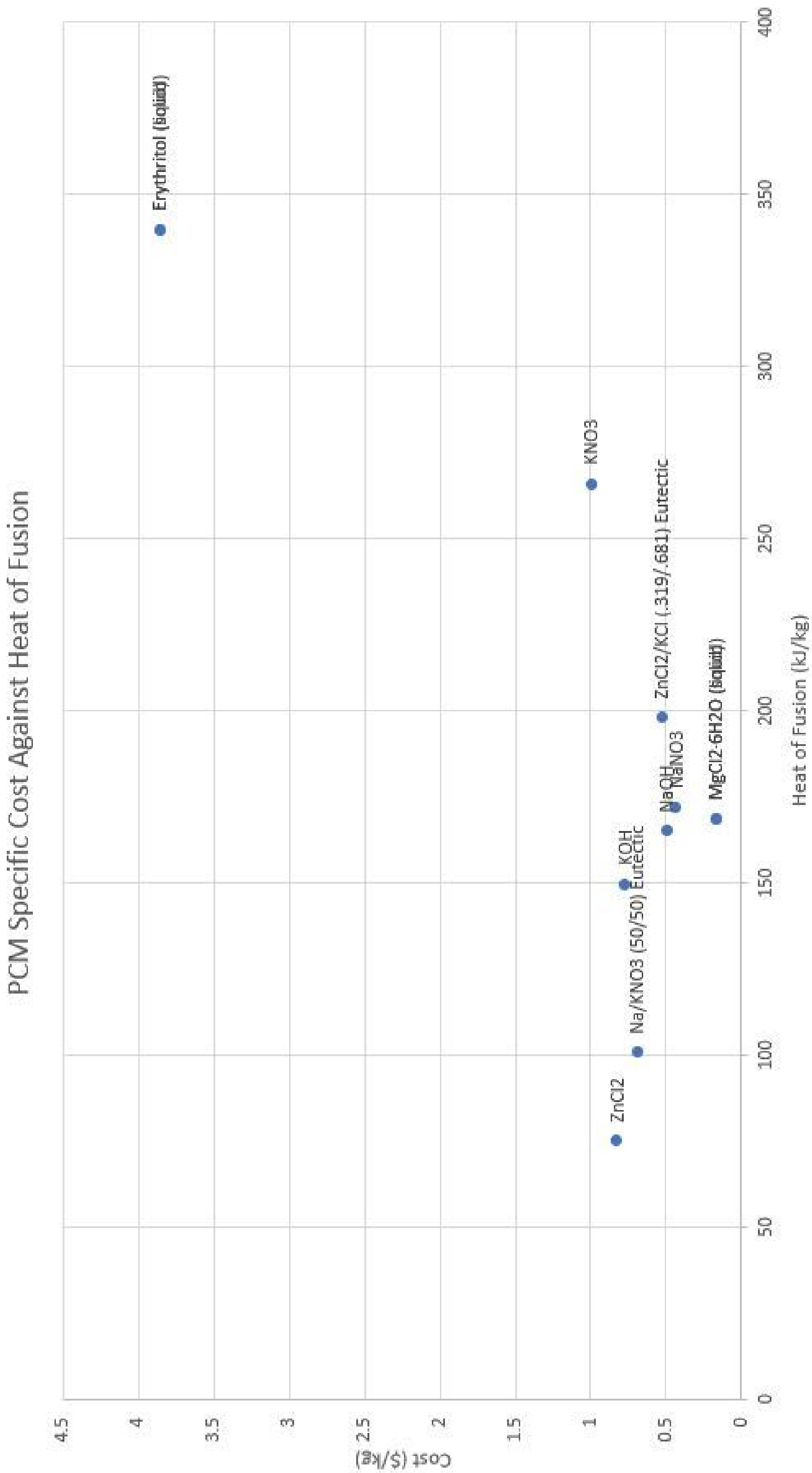

Figure 8. Cost of TESM vs. Heat of Fusion.

Ideal TESMs should have low cost and high heat of fusion. Unfortunately, many otherwise suitable TESM salts are too expensive to realistically consider using, and so they aren't included. Per kilogram, erythritol, a sugar alcohol, is the most expensive material, but also the most potent with the highest heat of fusion at nearly 350 kJ/kg. However, there are a multitude of problems in its use. Besides its prohibitive cost, erythritol's organic nature will make it likely to oxidize at high temperatures, particularly in contact with heating elements, and its melting point is too low for optimal steam production or heat transfer. The cheapest material is MgCl2-6H2O, and it's heat of fusion is near the middle of the pack with around 170 kJ/kg.

For our model, we determined potassium nitrate (KNO_3) to be the most cost effective material. Although its price is high relative to comparable ionic salt TESMs, a significantly higher heat of fusion of 266 kJ/kg as well as a higher melting point make it a cost efficient, and energy dense TESM option with appropriate melting points for steam generation and energy conversion. Although nitrate salts are known to cause corrosion issues in potential metal housing such as copper and steel, high temperature polymer linings will prevent degradation of metal containers--and KNO_3's lower melting point compared to other salts allows for these polymer linings to be used within their operating temperatures. Thus, for consistency and to model a flexible-use salt, we have made our model using KNO_3 as the TESM.

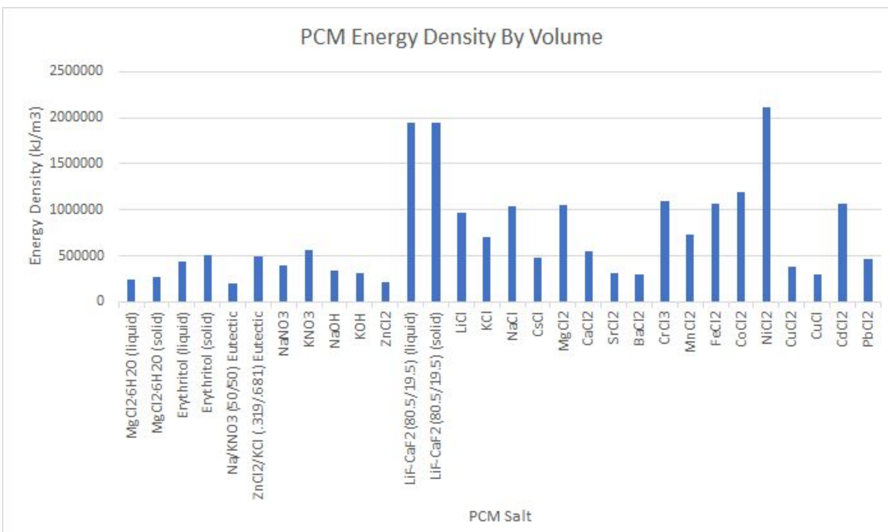

Figure 9. Energy Density of potential TESMs

Energy density by volume is also a relevant factor. In situations where a municipal storage system local to power generation sites will be delivered, or real estate will be limited, more energy dense salts will be needed. The two most energy dense salts by volume are LiF-CaF_2 eutectics and $NiCl_2$. Although both are similar in energy densities, LiF-CaF_2 eutectics are prohibitively expensive at $181/kg, while $NiCl_2$ is about $26.70/kg, although $NiCl_2$ has a slightly lower heat of fusion at 595 kJ/kg when compared to LiF-CaF_2 eutectic's 816 kJ/kg. The price difference between the two salts leaves $NiCl_2$ the best option for areas where real estate is a problem, although its price is significantly higher than our chosen salt of KNO_3. The cost of

$NiCl_2$ alone pushes thermal to be a wholesale storage technology where unit volume and area are not problems.

4.3.3.2. Insulation Analysis

Noteworthy insulation materials have a low thermal conductivity, while having a high maximum service temperature. This ensures that the insulation material will not conduct heat or degrade at high temperatures, limiting heat loss from the TES unit. For our findings, we found several different insulation materials that fulfilled these requirements, listed on table 7.

Classification	**Material**	**Continuous Use Temp (deg C)**	**Maximum Service Temp (deg C)**	**Temp ranges for Corresponding Material Properties (deg C)**	**Thermal Conductivity (W/(m*k))**	**Cost ($/m3)**
Refractory Concrete	Kast-o-Lite 22 PLUS	815	1205	205	0.250	5626.69
Aerogel Blanket	Pyrogel XTE	600	650	200	0.028	51964.00
Ceramic Fiber	Cerachrome	1370	1427	260	0.060	35777.39
Firebrick	K-23 Firebrick	1704	1915	260	0.170	43420.49

Table 6. Insulation Material comparison.

It was found, however, that none of these materials can be used alone in the context of the TESM tank. Aerogel, ceramic fiber, and firebrick all have lower thermal conductivities than refractory concrete, but they are also all porous and would be dangerous to use alone in containing the TESM - particularly as it liquifies. Using a mixture of each of the materials is necessary. Rather than determining a specific composition of insulation, our model follows an average insulation thermal conductivity of 0.1 W/(mK). In practice, this insulation would require a “container” of refractory concrete or steel as a non-porous high-temperature vessel for the molten salt. Use of either is dependent on material interactions, as some ionic salts may degrade oxides found in refractory concretes [9]. Surrounding this vessel would be a combination of the other three insulation materials, where small amounts of firebrick would surround the vessel to ensure continuous use temperatures of the ceramic fiber and aerogel are not exceeded. Because aerogel blankets and ceramic fiber are below the 0.1 W/(mK) threshold, more of them will be used to bring the weighted average of thermal conductivity for all insulation to the threshold. Since aerogel isn’t produced on a mass scale because of its manufacturing methods, more ceramic fibers must be used in its place. When determining capital cost of materials, deciding the proper composition of insulation is pertinent. Aerogel is vastly expensive relative to ceramic fiber. As such, use of ceramic fiber will likely be a common solution to energy storage solutions that have a limited budget. However, in higher budget situations where real estate is limited, aerogel’s low thermal conductivity will outperform the ceramic fiber, so heavier, though not complete, reliance on it will be necessary.

4.3.4. National Grid Fixed Peak/Off-Peak Analysis

Currently, energy storage is an expensive endeavor. Our models compare 1MWh of effective storage in our modeled thermal energy storage as well as the current lithium-ion storage. We based our first analysis on National Grid's peak/off-peak pricing models rather than traditional peak shaving models to minimize loss due to length of storage time. Because of National Grid's set peak/off-peak hours of 8:00am to 9:00pm for peak hours and 9:00pm to 8:00am for off peak hours, charging times are set to be as soon as possible before the pricing switch at 8:00am, and discharge times are set to be the same after the pricing switch at 8:00am. [53] Assuming a charge and discharge rate matching WPI's consumption at the respective times, this aims to limit energy loss in our modeled thermal battery, although this also limits a negligible amount of loss in lithium-ion batteries as well.

Our analysis follows 4 months, each representing a respective season. January, April, July, and October each represent winter, spring, summer, and fall respectively. We have analyzed WPI's consumption during each month by modeling the average day of each month. Analyzing and graphing each of the months' average days results in the following information regarding WPI's seasonal consumption differences.

	January 2019	**April 2019**	**July 2019**	**October 2019**
Peak Consumption (kW)	1234	1380	1670	1928
Trough Consumption (kW)	883	908	848	1149
Peak Time	12:12	14:18	14:27	13:27
Trough Time	2:03	1:57	3:45	2:36

Table 7. Peak Consumption by Season

This consumption data is particularly relevant in reference to prices. If prices during each of these months are particularly high during peak consumption hours, then peak shaving will be significantly more effective due to the higher prices avoided. However, since National Grid utilizes fixed peak/off-peak pricing at fixed times, consumption rate does not affect pricing--only storage capacity does. We have modeled and analyzed around a 1 MWh effective storage capacity, meaning after efficiency losses, the modeled batteries will be able to discharge 1MWh.

Peak consumption is during our modeled "average day" in October, likely due to heating bills in residential halls during the academic year, while lowest consumption is during January, likely because a large portion of it is during the academic winter break. Consumption peaks during the afternoon and falls to its lowest in the middle of the night, as expected based on when the campus has the greatest and least loads based on natural campus activity.

When profits are calculated, we begin to understand that storage at the scale of 1MWh of effective storage is far too small to reap profit. Based on our models, profits for each month in thermal batteries follow total storage time, energy conversion efficiency, and total capacity. For each month, thermal battery profits are as follows, where dark red and dark green indicate discharge and charge cycles respectively.

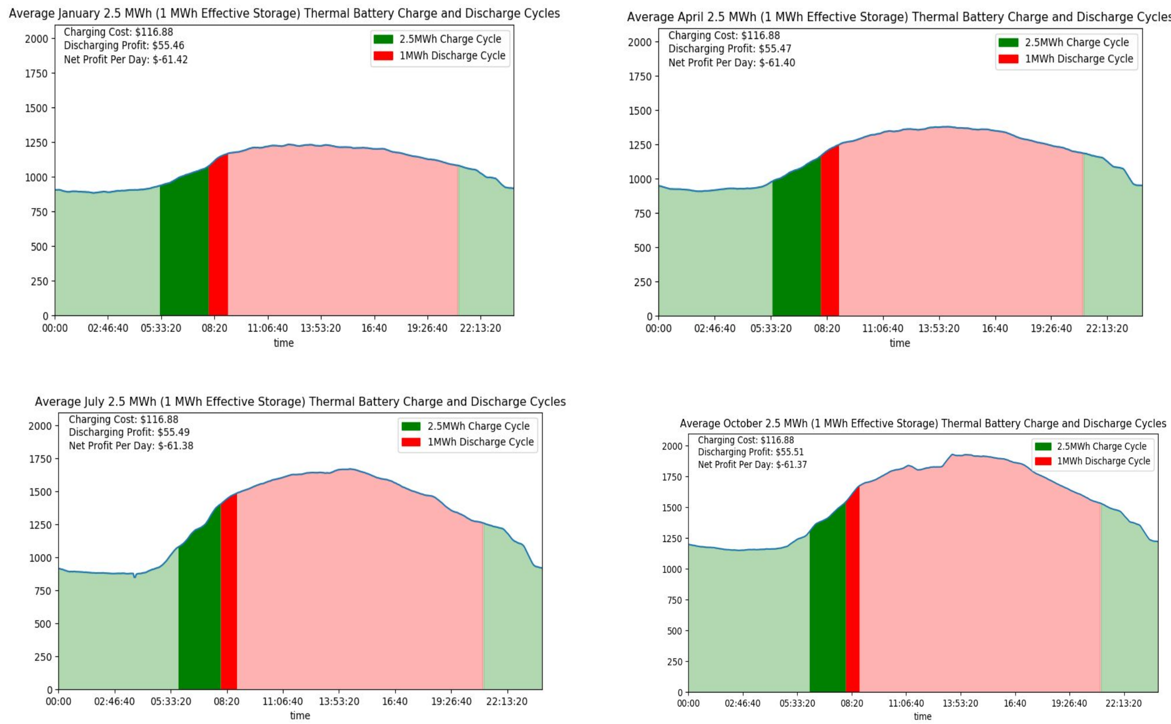

Figure 10. Average Seasonal Daily Power Consumption, with Average TES Storage Profits for Each Month

	January	**April**	**July**	**October**
Peak Consumption (kW)	1234	1380	1670	1928
Trough Consumption (kW)	883	908	848	1149
Peak Time	12:12	14:18	14:27	13:27
Trough Time	2:03	1:57	3:45	2:36
Average Loss in Thermal Over Storage Period (% Capacity/day)	0.026	0.025	0.023	0.021
Average Thermal Profit Per Day ($/day)	-61.42	-61.40	-61.38	-61.37
Average Loss in Lithium-Ion Over Storage Period (% Capacity/day)	0.595	0.561	0.493	0.433
Average Lithium-ion Profit Per Day ($/day)	-0.77	-0.77	-0.77	-0.77
Time Stored (h)	3.7	3.55	3.25	3

Table 8. Average loss in Capacity over Storage Period. Storage Period Defined as Charge Time Plus Discharge Time.

According to the analysis, consistently and across all seasons, there is significant capital loss per day when the modeled TES system is used. Profits are calculated taking storage cost and discharge profits into account. This involves efficiency as well as energy loss to the atmosphere over the period of storage. Because National Grid's peak/off-peak pricing program is fixed, there is a specific minimum efficiency threshold required to profit. This minimum efficiency for break-even is equal to the ratio of off-peak to peak prices. Using National Grid's pricing, this means that the minimum efficiency for storage to break even using National Grid's pricing model is:

$$\frac{.05428\ \$/kWh}{.04675\ \$/kWh} = 0.861\ efficiency = \ 86.1\%\ efficiency \tag{15}$$

Because the thermal battery model's theoretical maximum (Carnot) efficiency calculated using the melting point of KNO_3 is only 40% for energy conversion, even while assuming zero energy loss over time, it is not possible to profit from the modeled thermal battery system under this pricing system and system parameters.

We also ran this same consumption data using National Grid's pricing model while analyzing current lithium-ion storage parameters for efficiency and efficiency loss. Because there is virtually no energy loss over time, with about a 0.17% stored energy loss per hour, we calculated that there is nearly no difference in profits from month to month when using lithium-ion since the loss over the storage period is negligible. Since profits are effectively only determined by storage capacity and price differences, profits can be accurately modeled from month to month using simple arithmetic. For the purposes of comparison with TES however, the following represents a given month's charge and discharge cycles as well as profits if lithium-ion is used in this form of "peak shaving".

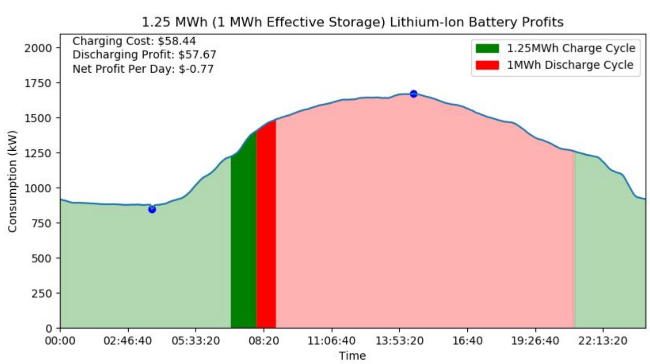

Figure 11. Average Daily Power Consumption

As is clear here, there are still slight losses when using lithium-ion at this scale and efficiency. The modeled lithium-ion battery here is assumed to be 85% efficient as commercial lithium-ion batteries are estimated to be between 80-90% efficient. This 85% efficiency is slightly under the 86.1% minimum required for breakeven. A slightly more efficient battery may result in either break-even or minor profit, but even current lithium-ion technologies under this pricing model is still not usable. The most efficient lithium-ion batteries will still not produce enough profit to pay off their initial investment cost in a reasonable amount of time.

It is worth noting, however, that a properly insulated TES unit shows significantly less profit loss per day relative to lithium-ion, in a context where thermal bridging effects are not accounted for, and the tank is assumed to be solely surrounded by air. Given TES's ability to recharge consistently and with little degradation of storage capacity (except to overheating, depending on the PCM), if a more efficient thermal energy conversion method is applied to TES, it can outperform lithium-ion in this regard.

4.3.5. Real Time ISO Data Analysis

True real-time electricity pricing usually involves live prices that are updated every handful of minutes. These prices are dictated by a central independent system operator (ISO). On the east coast, the New England (NE) ISO determines the prices for wholesale electricity. Similar to the National Grid pricing, we created an average day of the same four months in terms of the pricing provided by the ISO. Because the ISO only provides the price of electricity itself, we also normalized the ISO pricing data for electricity transfer cost by using modifiers provided by National Grid. Our analysis is built on these assumptions, so understanding that transfer fees (among others) will differ between utility providers is expected.

The NE ISO provides Locational Marginal Pricing (LMP) based on the wholesale market at a given time, meaning energy prices will differ based on supply and demand within the entirety of New England; this is analyzed every five minutes and the ISO releases pricing data following this interval as well. We average all of the values of LMPs for a month into one "average day" in a respective month. This naturally smooths for local changes in weather but also accounts for large storm systems and patterns which may affect the region during respective seasons. "Average days" in January, April, July, and October 2019 are graphed below.

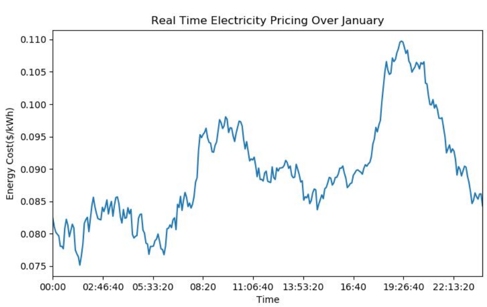

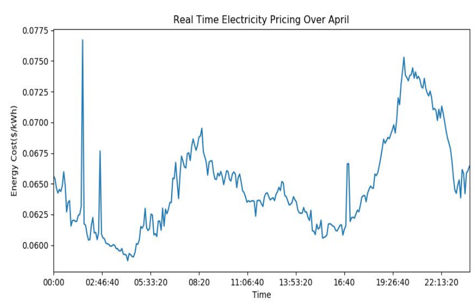

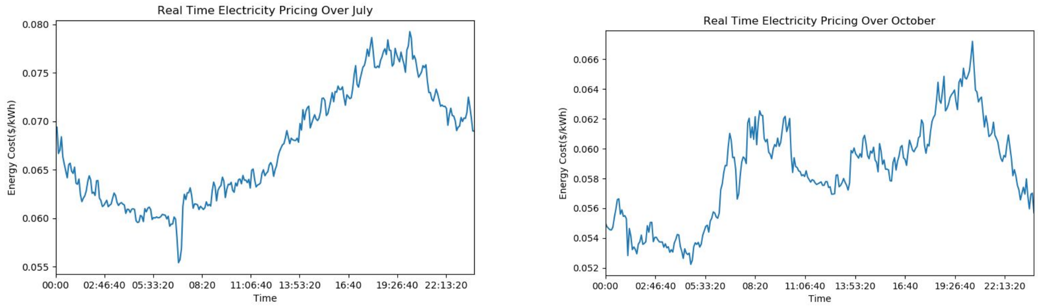

Figure 12. Real Time Seasonal Pricing

	January	April	July	October
Peak Price ($/kWh)	0.1097	0.0767	0.0792	0.0672
Trough Price ($/kWh)	0.0751	0.0587	0.0554	0.0522
Trough/Peak Price Ratio	0.685	0.766	0.699	0.777
Average Price ($/kWh)	0.09	0.065	0.067	0.058
Peak Time	19:20	20:03	20:10	20:25
Trough Time	1:30	4:15	7:00	4:45

Table 9. ISO NE Data Normalized with NG Transport Charges.

The most relevant data to our analysis here is the trough/peak price ratio for each month. This ratio represents what percent of the peak price the trough price is. In essence, it is the minimum efficiency for break-even in a pricing system similar to National Grid's fixed off-peak/peak pricing--where the peak pricing is fixed at the peak price of the average day, and the off-peak pricing is fixed at the trough pricing of the average day. This is not accurate to the true real time pricing, but is instead the best case scenario in terms of profit.

As seen in across all months, the average trough/peak price ratios do not drop below 0.685, which represents a minimum battery efficiency for profit of 68.5% in the most ideal pricing scenario. Even with the largest price disparities over the day, our modeled thermal battery's efficiency of 40% will still result in significant loss each day if used for peak shaving--and this is not accounting for the now additional heat loss to the atmosphere due to longer storage periods between the peak and trough prices.

Under lithium-ion's projected efficiency range of 80-90% (or our calculated 76%), these trough/peak price ratios indicate the possible profit. However, because we are assuming the absolute ideal pricing scenario, and the required efficiencies are close to true lithium-ion efficiency, in the majority of true real time pricing situations, lithium-ion could fare similarly in terms of resulting in either loss, or in profits too small to pay off a large investment cost. Automatic response throughout the day can regulate charging and discharging of lithium-ion batteries, so it can benefit from short term storage and discharge situations; thermal batteries are limited in its possible response time due to their reliance on steam turbines for conversion from thermal to electrical energy.

4.3.6 Heat Recycling From Thermal Energy Storage Units

Recycling heat from stored thermal energy is a huge selling point of TES, given its ability to raise the unit's efficiency as long as waste heat from energy conversion is properly utilized. In practice, heat from the steam turbine exhaust would be diverted to either a water or furnace based heater. Because the vast majority of WPI's buildings utilize water-based heating systems, rather than air-based furnace heating systems, a heat recycler in WPI's context would involve a heat exchanger between the output liquid-vapor mixture from the unit turbine and a flow of water. This water would then flow to an insulated tank for storage, or directly flow to buildings for use. Because the heat exchange would be through a simple heat exchanger, the only realistic loss would rise from insulation limitations/loss to the atmosphere.

Because heat recycling repurposes energy that was not converted by the steam turbine, properly recycling all of the waste heat could lead to a theoretical 100% system efficiency. The possible amount of recoverable heat is equal to the heat lost to lack of turbine efficiency and atmospheric loss from the TESM tank:

Assuming no atmospheric loss :

$$Recoverable\ Heat\ =\ TES\ Unit\ Capacity\ *(1-TES\ Unit\ Efficiency) \quad (16)$$

$$Recoverable\ Heat\ = 1.5\ MWh\ = 2.5\ MWh\ *(1-0.40)$$

Because WPI's buildings utilize natural gas heating for the majority of buildings, comparing recovered heat to possible savings in reference to natural gas is logical. Natural gas in the United States is sold in units of US Therms per unit price. The total recoverable heat in therms is represented as:

$$Recoverable\ Heat\ =\ 1.5\ MWh\ \frac{1000\ kWh}{1\ MWh}\frac{1\ Therm}{29.3\ kWh}\ =\ 51.19\ Therms\ per\ full\ TES\ unit\ charge \quad (17)$$

However, this would only be relevant during months where heating would be necessary, allowing this heating co-storage to occur during fall and winter months. This heating would also require huge amounts of campus infrastructure changes, as the heated water would need to be delivered in an insulated pipe to each building that would require heating. Creating a system for insulated liquid transfer would require significant time and capital investment.

Although water heated via this method can be stored, not all of it will be needed to heat buildings, and some will inevitably go to waste. It can be assumed that only fractions of this ideal recyclable heat will be used per charge, which will affect cycle efficiency differently. Heat recycling will likely be heavily involved in determining TES's niches.

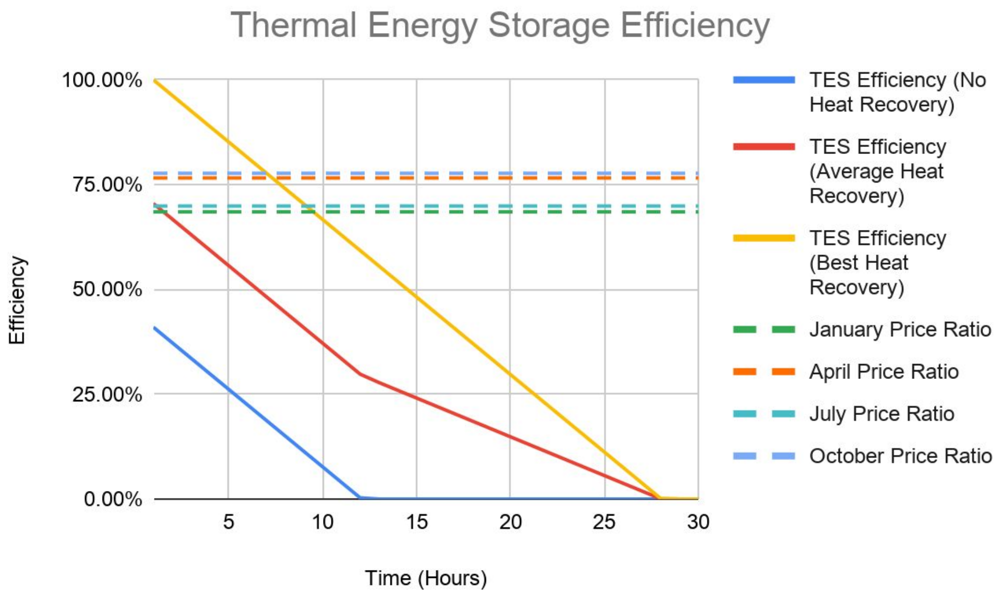

Figure 13. TES Energy Storage Efficiency**.**

4.3.7. Lithium Ion Comparison

Lithium-ion's efficiency is also significantly reduced due to the fact transmission and main power is an AC signal. As lithium ion batteries can only store DC signals, any power would need to be converted from ac to dc, stored, then converted from dc to ac. While none of these factors are low efficiency innately, they each work to lower the total efficiency of a lithium based system. In the best care scenario, low power ac to dc converters have an efficiency of 90% [45] and dc to ac has a best efficiency of 97% [46]. This makes the total immediate efficiency of lithium 86.4% at best. At worst care, AC to DC and DC to AC have an efficiency of 75%. This makes the total immediate efficiency 55.7%. Combining this with the real time energy data gathered above creates this graph.

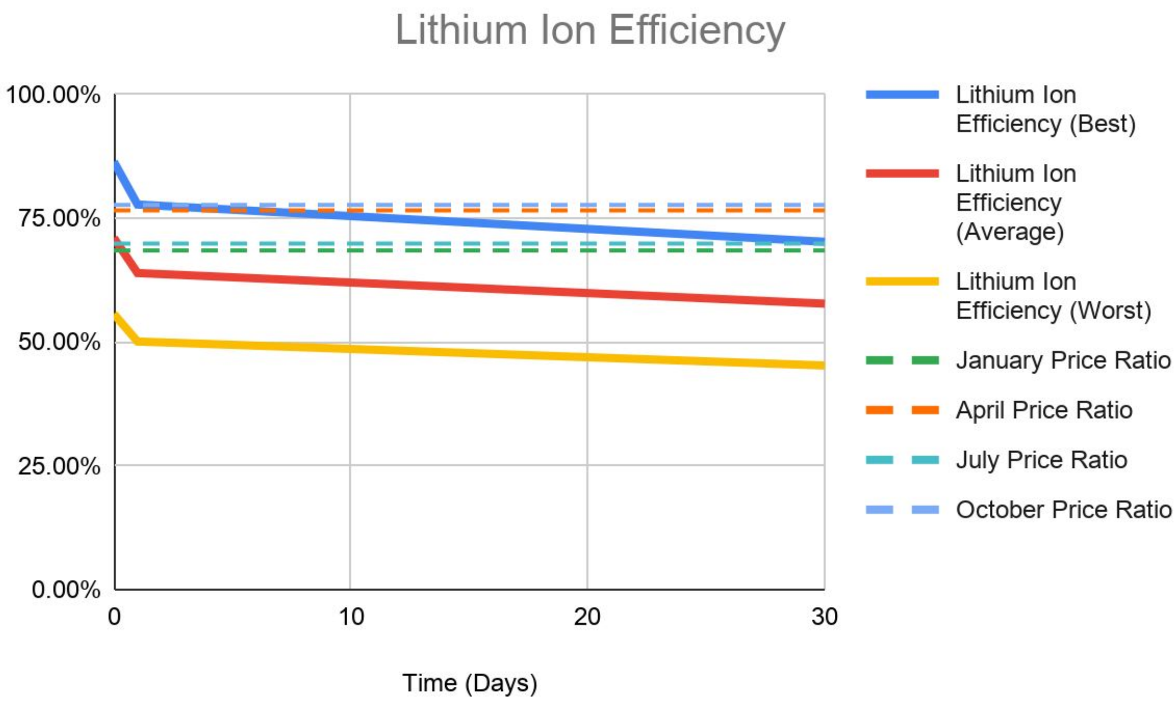

Figure 14. Lithium Ion Efficiency Per Day

As the graph shows, any attempt to capitalize on the changing price over the day could work with a very ideal lithium ion battery setup, but on average cannot turn a profit given the most ideal scenario. This scenario also ignores the fact that the peaks and trough are only at these prices for very slim amounts of time, and would thus need to pull an extremely large amperage which would quickly damage the lithium ion batteries. It should also be noted again that purchasing electricity and storing it when the efficiency is below the price ratio means that the electricity would cost more to buy and store than to buy at the peak time per watt. The option of buying power while the price is low and using it while the price is high, is also not realistic with current efficiency ratings of energy conversion.

5. CONCLUSIONS

To appropriately understand the use cases of thermal energy storage (TES) when compared to current lithium-ion storage technologies, we used multiple tools to enable a holistic analysis of each technology when used in the context of the current energy market.

The design of a thermal energy storage unit built around WPI's consumption needs was used as a test case in order to compare it to widely used Lithium-ion batteries. Analysis of possible thermal storage media used for latent energy storage (as seen in many similar units), as well as possible insulation materials were involved in determining input parameters of the model to ensure accuracy against a comparable built unit.

Calculated efficiencies and losses from the modeled thermal unit as well as equivalent researched parameters in Lithium-ion were used for market analyses in two different energy pricing models. The first model was the current local energy pricing scheme, which follows a fixed off-peak/peak pricing model at times set by National Grid specifically for sources that draw power at rates greater than 200kW. The second more ubiquitous model that follows real-time pricing, which is recalculated every 5 minutes by the New England ISO, which regulates the wholesale energy market.

5.1. TESMs and Insulation

To create an effective TES, a stable and cheap thermal energy storage material is required, as well as a good insulation material. A good TESM is paramount for unit cost, capacity, and volume, and a higher heat of fusion allows for more latent energy storage per unit mass. Looking at the data for the price of TESMs compared to their heat of fusion:

We found potassium nitrate (KNO_3) to be the most cost effective material. While it may have a relatively expensive price, it has a significantly higher heat of fusion of 266 kJ/kg as well as a higher melting point which makes it cost efficient relative to the other potential TESMs. Additionally, it is an energy dense TESM option with appropriate melting points for steam generation and energy conversion.

Aerogel blankets are the most effective insulation, but are orders of magnitude more expensive than refractory concrete, our cheapest option. Aerogel blankets are 2.14 times more effective than ceramic fiber in reference to thermal conductivity, and 1.45 as expensive, leaving aerogel as more cost effective than the next best option. However, if initial capital cost must be limited and real estate not, then heavier use of ceramic fiber and less use of solid-conductive insulation (in refractory concrete and firebrick) can ease budgetary pressure while maintaining similar (though not equivalent) insulation effectiveness.

As is common, the "best" insulation is heavily dependent on context. Cost, system volume, pricing model, and container surface area are all relevant in determining how long energy needs to be stored for, the service temperatures of the insulation, cost of insulation, and amount of insulation needed for system capacity. In an ideal scenario, high temperature aerogel blankets surrounding a concrete vessel create the most effective insulation, but given the low production velocity and scale of high temperature aerogel solutions, ceramic fiber is an economic, realistic, and our recommended alternative given its significant edge price-wise, and similarly low thermal conductivity.

5.2. Thermal Battery

It is also possible to conclude from the modeling of the thermal battery that this type of model is unlikely to be efficient enough to be implemented as a profitable TES device, unless the heat lost in conversion is used for heating purposes on the campus buildings as well. It is also worth mentioning that while we assume the simulation of the model is realistic, it is by far not a complete model, and that a more professional assessment could be made in order to provide a better program that simulates heat flow inside the unit, leading to a more successful design.

Another shortcoming of this design lies on the practical implementation of this design. While this device was not actually built, it is possible to foresee possible problems based on a concept developed by a small thermal energy storage startup named Terrafore Technologies [source]. Founded by engineer Anoop Marthur in Minnesota, Terrafore Technologies pioneered the development of an “Active Heat Exchanger PCM TES” unit using a dilute eutectic composition, but concluded that while the concept was innovative and was proven to be used to create a battery with a large energy density, several practical problems encountered made the implementation cumbersome and inefficient. A major issue encountered was the solidification of salt onto heat exchanger surface and thus decreasing the heat transfer coefficient. A solution for this problem made by the company was to use salt-phobic coating on the surface of the heat exchanger to reduce this, but this led to the other issues. At the end, the company decided that these efforts were not sufficient, and decided to cancel the project. This is evident from the following excerpt taken from the company’s website:

“Terrafore determined that there are many engineering risks to scale this system. The benefit of 30% improvement in energy density gained by using phase change does not pay for the additional expense to protect the system using trace heaters for the entire system. Any blockage of salt in the tubes will require expensive repair. Therefore, Terrafore recommended that the development be stopped during Phase 2 of the project…”

However, the company acknowledges that this enterprise was not a complete failure nonetheless, as it was possible to learn from these in order to build better TES storage energy devices. Similarly, we believe the design and implementation of this unit have led us to learn lessons that can be used for next projects involving the implementation of TES units.

5.3. Market Analysis

5.3.1. Market Analysis (Fixed Off-Peak/Peak Pricing)

Following National Grid's pricing model and WPI's consumption data over 4 months--January, April, July, and October--each representing winter, spring, summer, and fall respectively--TES falls significantly short of profit in each month, while lithium-ion--while still falling short--results in very little loss, but loss nonetheless.

	January	April	July	October
Average Thermal Profit Per Day ($/day)	-61.42	-61.40	-61.38	-61.37
Average Lithium-ion Profit Per Day ($/day)	-0.77	-0.77	-0.77	-0.77

Table 10. Average Energy Storage Profit per Season

Averaging losses around $75 per day places TES in a spot where significant design overhauls involving conversion efficiency improvement are required. Because lithium-ion's average profit loss is under a dollar per day, a battery with slightly higher efficiency could reach break-even or profit. However, since the 85% efficiency we assumed for lithium-ion is only 5% off from the current peak for lithium-ion of 90% efficiency, possible profits would be very limited and given that lithium-ion's investment cost is currently the limiting factor in its use, we advise against WPI using either of these technologies for peak shaving under National Grid's fixed off-peak/peak pricing models.

5.3.2. Market Analysis (Real Time Pricing)

Real-time pricing is a more robust model for electricity pricing as dependence on intermittent renewables increases. We utilized the real time pricing the New England ISO provides on their website, which is updated every 5 minutes, rather than National Grid's fixed price and fixed time pricing changes. To justify our recommendations, we assumed the most ideal scenario to determine possible efficiencies for profit. We determined the average peak and average trough prices, and took the ratio between the trough and peak prices. The ratio between the two prices indicates the minimum efficiency required for break-even assuming the prices are fixed at the peak price during peak hours, and the trough price during off-peak hours, similar to the National Grid model.

	January	April	July	October
Peak Price ($/kWh)	0.1097	0.0767	0.0792	0.0672
Trough Price ($/kWh)	0.0751	0.0587	0.0554	0.0522
Trough/Peak Price Ratio	0.685	0.766	0.699	0.777

Table 11. Peak/Trough Price Ratio per Season

Under both pricing models, it was found that thermal energy storage units, in the context of WPI's usage and following our model, will not result in profit under either pricing model. lithium-ion fares similarly under National Grid's fixed pricing model, with slight net loss each day. The only case where profit is reasonable is lithium-ion in a real-time pricing model, mirroring the current use of lithium-ion in peak shaving.

5.3.3. Heat Recycling

Heat recycling poises TES as a genuinely useful technology. While all other market analyses point to TES leading to significant losses, the use of heat recycling vastly increases the efficiency of TES units when it is relevant. In the context of the colder months, heat recycling is a very useful second use of the energy storage unit. With perfect utilization of heat recycling, the TES unit's efficiency can theoretically reach 100%. Although unrealistic, even 50% utilization of lost energy in heat recycling places TES's efficiency around 70%, nearing lithium-ion's efficiency. 75% heat recycling utilization places TES's efficiency at 85.5%, exactly in the range as the most efficient lithium-ion units. If utilized properly, heat recycling leaves TES in a favorable position economically. It is also a significantly greener source of heating, as the original heat source comes from electrically resistive heating, which bypasses the need for natural gas combustion, a common fuel source for heating systems at WPI.

However, heat recycling is severely limited, as it can only be used when buildings need to be heated. During summer months, heat recycling is nearly irrelevant and will unlikely be able to drive up efficiency to a degree where it is profitable. Determining true profit will depend on WPI's heating costs--specifically costs for natural gas in $/Therm. Calculating exact profit will be contextual. Thus, TES units properly utilizing heat recycling during winter months could match the efficiency of current lithium-ion technologies at a fraction of the initial cost.

5.3.4. Lithium-ion Comparison

Based on our results, thermal energy storage technology fills a complementary role compared to lithium-ion. Thermal energy is not viable for any small power or small scale applications. Yet, it may still be considered to large power applications, particularly as a energy storage/heating unit and in heat recycling to increase its efficiency. Additionally, since lithium-ion fails at high amperage and temperature ranges, thermal energy storage is more likely to be implemented as a more viable solution in places with high temperatures year-long. We therefore predict there should be ample market opportunities for TES in these two areas in which lithium-ion cannot be efficiently implemented. However, on WPI's storage scale, according to our calculations lithium-ion is a significantly better choice, unless better materials or more accurate modelling show that it is possible to make a TESU in which it is possible to ue up to 80% of the total energy stored as either electricity or heat.

lithium-ion also cannot be used to maximise savings from real-time energy pricing. Optimal price ratios are only slightly lower than the highest efficiencies found in lithium-ion batteries. Ongoing research in different energy storage solutions must still be carried out in order to create devices that enable profitable large-scale energy storage to successfully transition our society to fully rely on intermittent renewable energy sources.

6. REFERENCES

1. Sarbu, Ioan, and Calin Sebarchievici. "A Comprehensive Review of Thermal Energy Storage." Sustainability, 14 Jan. 2018, DOI: 10.3390/su10010191.
2. Medved, Dusan, et al. "Latent Heat Storage Systems." *ZCU.cz*, May 2010, https://pdfs.semanticscholar.org/6b74/2da25be1dd90469fabc12fbafb5a1847eb7d.pdf
3. Marína José, and Luisa F. Cabeza. "Review on Thermal Energy Storage with Phase Change: Materials, Heat Transfer Analysis and Applications." *Applied Thermal Engineering*, Pergamon, 6 Dec. 2002, DOI: 10.1016/S1359-4311(02)00192-8 https://doi.org/10.1016/S1359-4311(02)00192-8
4. Y. Tian et al. "A Review of Solar Collectors and Thermal Energy Storage in Solar Thermal Applications." *Applied Energy*, Elsevier, 22 Dec. 2012, DOI: 10.1016/j.apenergy.2012.11.051.
5. Bosschea, Peter Van den, et al. "SUBAT: An Assessment of Sustainable Battery Technology." *Journal of Power Sources*, Elsevier, 22 Aug. 2005, DOI: 10.1016/j.jpowsour.2005.07.039 www.sciencedirect.com/science/article/pii/S0378775305008761.
6. Fu, Ran, et al. "2018 U.S. Utility-Scale Photovoltaics-Plus-Energy Storage System Costs Benchmark." *Nrel.gov*, National Renewable Energy Laboratory, Nov. 2018, www.nrel.gov/docs/fy19osti/71714.pdf.
7. Ziegler, Micah S., et al. "Storage Requirements and Costs of Shaping Renewable Energy Toward Grid Decarbonization." *Sciencedirect.com*, Joule, 18 Sept. 2019, www.sciencedirect.com/science/article/abs/pii/S2542435119303009.
8. Paksoy, Halime O. "Thermal Energy Storage for Sustainable Energy Consumption." *Springer.com*, NATO Science Series, July 2005, link.springer.com/content/pdf/10.1007%2F978-1-4020-5290-3.pdf.
9. Agyenim, Francis, et al. "A Review of Materials, Heat Transfer and Phase Change Problem Formulation for Latent Heat Thermal Energy Storage Systems (LHTESS)." *Renewable and Sustainable Energy Reviews*, Pergamon, 5 Nov. 2009, www.sciencedirect.com/science/article/pii/S1364032109002469.
10. Cabeza, L.F., et al. "Introduction to Thermal Energy Storage (TES) Systems." *ScienceDirect*, Woodhead Publishing, 7 Nov. 2014, www.sciencedirect.com/science/article/pii/B9781782420880500018.
11. Kreutzer, Cory, et al., "Design and Implementation of a Thermal Load Reduction System for a Hyundai Sonata PHEV for Improved Range." *Https://Www.nrel.gov/Docs/fy18osti/70656.Pdf*, 3 Apr. 2018, www.nrel.gov/docs/fy18osti/70656.pdf.
12. Ziegler, Micah S., et al. "Storage Requirements and Costs of Shaping Renewable Energy Toward Grid Decarbonization." *Sciencedirect.com*, Joule, 18 Sept. 2019, www.sciencedirect.com/science/article/abs/pii/S2542435119303009.
13. Glatzmaier, G. "Developing a Cost Model and Methodology to Estimate Capital Costs for Thermal Energy Storage." *Nrel.gov*, National Renewable Energy Laboratory, Dec. 2011, Ziegler, Micah S., et al. "Storage Requirements and Costs of Shaping Renewable

Energy Toward Grid Decarbonization." Sciencedirect.com, Joule, 18 Sept. 2019, www.sciencedirect.com/science/article/abs/pii/S2542435119303009.
14. Kariya, Jun, and Yukitaka Kato. "Development of Thermal Energy Storage Material Using Porous Silicon Carbide and Calcium Hydroxide." *ScienceDirect*, Elsevier, 28 Dec. 2017, www.sciencedirect.com/science/article/pii/S187661021734571X.
15. Nordell, Bo. "Large-Scale Thermal Energy Storage." *Stanford.edu*, Stanford University, 14 Feb. 2000, large.stanford.edu/courses/2013/ph240/lim1/docs/nordell.pdf.
16. Bernardi, Adriana, et al. "Adaptation of Energy Storage Systems to Cultural Heritage: the Applications of Phase Change Materials Technology to Historical Buildings and Objects." *ResearchGate*, Jan. 2013, www.researchgate.net/publication/261987740_Adaptation_of_energy_storage_systems_to_Cultural_Heritage_the_application_of_Phase_Change_Materials_technology_to_historical_buildings_and_objects.
17. Tielens, Pieter, and Dirk Van Hertem. "Grid Inertia and Frequency Control in Power Systems with High Penetration of Renewables." *SemanticsScholar*, pdfs.semanticscholar.org/1cd1/9e3ae4b3ff6919570cf6faa693a13d21652a.pdf.
18. Gyuk, Imre, et al. "Grid Energy Storage." *Energy.gov*, U.S. Department of Energy, Dec. 2013, www.energy.gov/sites/prod/files/2014/09/f18/Grid%20Energy%20Storage%20December%202013.pdf.
19. "Javascript Required!" *Molten Salt Reactors - World Nuclear Association*, World Nuclear Association, Dec. 2018, www.world-nuclear.org/information-library/current-and-future-generation/molten-salt-reactors.aspx.
20. Daley, D. J., and J. Haslett. "A Thermal Energy Storage Process with Controlled Input." *Advances in Applied Probability*, vol. 14, no. 2, June 1982, pp. 257–271.
21. Bonte, Matthijs, et al. " Underground Thermal Energy Storage: Environmental Risks and Policy Developments in the Netherlands and European Union." *Ecology and Society*, vol. 15, no. 1, Mar. 2011.
22. Kalhammer, Fritz R. "Energy-Storage Systems." *Scientific American*, vol. 241, no. No. 6, Dec. 1979, pp. 56–65.
23. "New CSP Funding Is Getting Hotter." *NREL.gov*, National Renewable Energy Laboratory, 29 May 2018, www.nrel.gov/news/program/2018/nrel-to-develop-third-gen-csp.html.
24. Cheralathan, M., et al. "Performance Analysis on Industrial Refrigeration System Integrated with Encapsulated PCM-Based Cool Thermal Energy Storage System." *Onlinelibrary.wiley.com*, International Journal of Energy Research, 12 Feb. 2007, onlinelibrary.wiley.com/doi/pdf/10.1002/er.1313.
25. Wang, Zhifeng. "General Design of a Solar Thermal Power Plant." *ScienceDirect*, Academic Press, 29 Mar. 2019, www.sciencedirect.com/science/article/pii/B9780128156131000031.
26. Liu, Changwei, et al. "A 500 W Low-Temperature Thermoelectric Generator: Design and Experimental Study." *ScienceDirect*, Elsevier, 23 Sept. 2014, www.sciencedirect.com/science/article/pii/S0360319914022095.

27. Wang, Zhongyong, et al. “Dynamic Tuning of Optical Absorbers for Accelerated Solar-Thermal Energy Storage.” *Nature News*, Nature Publishing Group, 14 Nov. 2017, www.nature.com/articles/s41467-017-01618-w.
28. "Molten silicon used for thermal energy storage". *The Engineer*. Archived from the original on 2016-11-04. Retrieved 2016-11-02.
29. Misra, Ajay. “Energy Conversion and Storage Requirements for Hybrid Electric Aircraft.” *Https://Ntrs.nasa.gov*, 27 Jan. 2016, ntrs.nasa.gov/archive/nasa/casi.ntrs.nasa.gov/20160010280.pdf.
30. “Electric Resistance Heating.” *Energy.gov*, U.S Department of Energy, www.energy.gov/energysaver/home-heating-systems/electric-resistance-heating.
31. Self, Stuart J., et al. “Geothermal Heat Pump Systems: Status Review and Comparison with Other Heating Options.” *Sciencedirect.com*, Elsevier, 11 Feb. 2012, www.sciencedirect.com/science/article/pii/S0306261912000542.
32. Buffa, S., et al. “5th generation district heating and cooling systems: A review of existing cases in Europe” Elsevier, Apr. 2019, https://reader.elsevier.com/reader/sd/pii/S1364032118308608?token=6F496B9BCA20442292F2AA1AA80C46883829088B92754D56762573719B72D72B541179B169651C1079E2AD04D2A7C84F
33. “ELECTRICITY STORAGE AND RENEWABLES: COSTS AND MARKETS TO 2030.” *IRENA*, IRENA, Oct. 2017, www.irena.org/-/media/Files/IRENA/Agency/Publication/2017/Oct/IRENA_Electricity_Storage_Costs_2017_Summary.pdf?la=en&hash=2FDC44939920F8D2BA29CB762C607BC9E882D4E9.
34. Serrano-López, R., et al. “Molten Salts Database for Energy Applications.” *Arxiv.org*, Plaza Misael Bañuelos, 17 Sept. 2013, arxiv.org/pdf/1307.7343.pdf.
35. Sohal, Manohar S., et al. “Engineering Database of Liquid Salt Thermophysical and Thermochemical Properties .” Https://Inldigitallibrary.inl.gov/Sites/STI/STI/5698704.Pdf, Idaho National Laboratory, June 2013, inldigitallibrary.inl.gov/sites/STI/STI/5698704.pdf.
36. Astin, A. V. “Molten Salts: Volume 1, Electrical Conductance, Density, and Viscosity Data.” *Nvlpubs.nist.gov*, U.S. Department of Commerce, Oct. 1968.
37. D’Aguanno, B., et al. “Thermostatic Properties of Nitrate Molten Salts and Their Solar and Eutectic Mixtures.” *Nature News*, Nature Publishing Group, 11 July 2018, www.nature.com/articles/s41598-018-28641-1.
38. “Combined Heat and Power Technology Fact Sheet Series.” *Https://Betterbuildingssolutioncenter.energy.gov/*, U.S Department of Energy, July 2016, betterbuildingssolutioncenter.energy.gov/sites/default/files/attachments/CHP-Steam%20Turbine.pdf.
39. Giguere, Jeremy, et al. “Energy Consumption of WPI Buildings.” *Https://Web.wpi.edu/*, Worcester Polytechnic Institute, 13 Mar. 2014, web.wpi.edu/Pubs/E-project/Available/E-project-031414-110432/unrestricted/energy-consumption-wpi-buildings.pdf.
40. “BU-802b: What Does Elevated Self-Discharge Do?” *Elevating Self-Discharge - Battery University*, Battery University, batteryuniversity.com/index.php/learn/article/elevating_self_discharge.

41. "Lithium-Ion Battery DATA SHEET." *Www.ineltro.ch*, EEMB Co., Ltd., www.ineltro.ch/media/downloads/SAAItem/45/45958/36e3e7f3-2049-4adb-a2a7-79c654d92915.pdf.
42. Chou, Chih-Chung, and Yen-Shiang Shih. "A Thermodynamic Approach to the Design and Synthesis of Plant Utility Systems." *Https://Pubs.acs.org/*, National Taiwan Institute of Technology, 1987, pubs.acs.org/doi/pdf/10.1021/ie00066a009.
43. Ohji, A., and M. Haraguchi. "Steam Turbine Cycles and Cycle Design Optimization: The Rankine Cycle, Thermal Power Cycles, and IGCC Power Plants." *Advances in Steam Turbines for Modern Power Plants*, Woodhead Publishing, 25 Nov. 2016, www.sciencedirect.com/science/article/pii/B9780081003145000026.
44. Myers, Philip D., and D. Yogi Goswami. "Thermal Energy Storage Using Chloride Salts and Their Eutectics." *Applied Thermal Engineering*, Pergamon, 7 July 2016, www.sciencedirect.com/science/article/pii/S1359431116311759.
45. Knowles, Don. "Understand Efficiency Ratings Before Choosing An AC-DC Supply." *StackPath*, ElectronicDesign, 26 Feb. 2013, www.electronicdesign.com/power-management/article/21795830/understand-efficiency-ratings-before-choosing-an-acdc-supply.
46. "6.5. Efficiency of Inverters." *6.5. Efficiency of Inverters | EME 812: Utility Solar Power and Concentration*, www.e-education.psu.edu/eme812/node/738.
47. Poullikkas, Andreas. "A Comparative Overview of Large-Scale Battery Systems for Electricity Storage." *Researchgate.net*, Cyprus University of Technology, Jan. 2013, www.researchgate.net/publication/258022527_A_comparative_overview_of_large-scale_battery_systems_for_electricity_storage.
48. Baker, R. "Battery Reality: There's Nothing Better Than Lithium-Ion Coming Soon" Bloomberg, 3 Apr. 2019, https://www.bloomberg.com/news/articles/2019-04-03/battery-reality-there-s-nothing-better-than-lithium-ion-coming-soon
49. Barrera, P. "Lithium Outlook 2020: The Lithium Decade Begins" Investing News Network, 8 Jan. 2020 https://investingnews.com/daily/resource-investing/battery-metals-investing/lithium-investing/lithium-outlook/
50. Schaefer, K. "Lithium Prices To Stay High To 2024–UBS" Oil and Gas Investments Bulletin, 6 June. 2017 https://oilandgas-investments.com/2017/top-stories/lithium-prices-to-stay-high-to-2024-ubs/
51. Roberts, D. "Getting to 100% renewables requires cheap energy storage. But how cheap?" Vox, 20 Sept. 2019 https://www.vox.com/energy-and-environment/2019/8/9/20767886/renewable-energy-storage-cost-electricity
52. Welty, Wicks, Wilson, Rorer. "Fundamentals of Momentum, Heat and Mass transfer'' 5th edition (Wiley, 2008). https://www.semanticscholar.org/paper/Fundamentals-of-momentum%2C-heat%2C-and-mass-transfer-Welty-Wicks/15632a2792afeed09f5516180a0932b83c088be1
53. "Time-of-Use Pricing for Industrial Customers." *Https://www9.Nationalgridus.com/*, National Grid, www9.nationalgridus.com/niagaramohawk/business/rates/4_tou.asp.

54. 1414 degrees,“SiliconAurora”.*(2020)*1414degrees.com.au/siliconaurora/.
55. University of Washington Clean Energy Institute “Lithium Ion Battery” (2020) https://www.cei.washington.edu/education/science-of-solar/battery-technology/
56. “Dresser-Rand Steam Turbines - a Siemens Business.” *Siemens.com Global Website*, Siemens, new.siemens.com/global/en/products/energy/power-generation/steam-turbines/d-r-steam-turbines.html.
57. Bergman, Theodore L., et al. *Fundamentals of Heat and Mass Transfer*. 7th ed., J. Wiley & Sons, 2011.

APPENDIX A: MATHEMATICA TESU UNIT MODELING PROGRAM

Program

```
(*                                              TES UNIT MODEL PROGRAM                                            *)
(*                                                By Federico Poggioli                                            *)

(*                                                   SI UNITS ONLY                                                *)

(* STEP 1: INSERT INITIAL PARAMETERS ------------------------------------------------------------------------------- *)
(* Set physical parameters *)
         (* Material Properties *)
         Kc      = 50.2;                (* Thermal Conductivity Steel *)
         HeatOfFusion  = 266000;        (* Heat of Fusion KNO3 *)
         Density = 2110;                (* Density KNO3 *)
         (* Temperature Conditions *)
         Twater        = 373;           (* 100 C, Water boiling point *)
         Tpipe         = 490;           (* 217 C, Assumed Initial Pipe temp *)
         Tpcm          = 607;           (* 334 C, PCM phase transition*)
         Tair          = 298;           (*  25 C, ambient temp *)
         (* Power Requirements *)
         PowerOut = 1*10^6;                      (* 1MW, WPI Power Consumption *)
         MaxEfficiency = N[1 - Tair/Tpcm];       (* Carnot Efficiency *)
         TurbineEfficiency = 0.4;                (* Turbine Efficiency < Carnot Efficiency *)
         PowerSteam = PowerOut/TurbineEfficiency; (* PCM Tank Power Output *)
         tDischarge = 1*3600;                    (* 1 Hour in seconds *)
         WorkSteam = PowerSteam*tDischarge;      (* 9*10^9 J, which is 2.5 MWh*)
         WorkIn = 0;                             (* Assume no pump is needed *)
         (* Device Dimensions *)
         L                      = 7.5;           (* PCM Tank Length *)
         WaterPipeInnerDiameter = 0.05;          (* Water pipe / Resistive material Pipe *)
         MetalThickness         = 0.01;          (* Steel Thickness *)
         (* Turbine Parameters *)
         TDrop   = 1;                   (* Turbine Temperature Drop *)
         Vf      = 1;                   (* Water/Steam Flow velocity *)
         (* Iteration Parameters *)
         length  = 10;                  (* Number of Length Divisions *)
         zfact   = L/length;            (* Length Iteration Factor *)
         time    = 60;                  (* Time Evaluation Parameter (60 seconds) *)
         tfact   = 60;                  (* Time Iteration Factor (60 min) *)
(* Data Parameters *)
         MaxDataRow = 80;               (* Excel table parameter *)
         MatNum     = 5;                (* Material Number - useful for Excel table iteration *)



(* STEP 2: CREATE TABLES AND RETRIEVE EXCEL DATA ------------------------------------------------------------------- *)
(* Define tables *)
         (* Temperature *)
         TWater  = Table[0,{z,length},{t,tfact + 1}];
         TPipe   = Table[0,{t,tfact+1}];
         TPCM    = Table[0,{t,tfact+1}];
         TAir    = Table[0,{t,tfact+1}];
         (* Heat *)
         QWater  = Table[0,{z,length},{t,tfact+1}];
         QPipe   = Table[0,{t,tfact+1}];
         QPCM    = Table[0,{t,tfact+1}];
         QAir    = Table[0,{t,tfact+1}];
         (* Length and Time*)
         zVal    = Table[0,{z,length}];
         tVal    = Table[0,{t,tfact+1}];
         (* Parameters from Excel file - These come from "Fundamentals of Momentum, Heat and Mass Transfer" 5th Ed. *)
         rho     = Table[0,{mn,MatNum}];
         cp      = Table[0,{mn,MatNum}];
         mu      = Table[0,{mn,MatNum}];
         nu      = Table[0,{mn,MatNum}];
         k       = Table[0,{mn,MatNum}];
         alpha   = Table[0,{mn,MatNum}];
         Pr      = Table[0,{mn,MatNum}];
         Grcoeff = Table[0,{mn,MatNum}];
         Gr      = Table[0,{mn,MatNum}];
         Ra      = Table[0,{mn,MatNum}];
         Nu      = Table[0,{mn,MatNum}];
         (* Other Physical Parameters *)
         h       = Table[0,{mn,MatNum}]; (* h is a convective heat transfer parameter to group many of these values *)
         F       = Table[0,{mn,MatNum}]; (* F is a parameter to group many of these values together *)
         A       = Table[0,{mn,MatNum}]; (* Surface Area *)
         CharL   = Table[0,{mn,MatNum}]; (* Characteristic Length *)
         Vol     = Table[0,{mn,MatNum}]; (* Volume *)
         (* Data Tables *)
```

```
        PM      = Table[0,{i,tfact + 1},{j,16}];
        DataRow = Table[0,{i,MaxDataRow}];
        Data    = MatrixForm[Table[
                                      Import["R:\\TESU IQP\TES_DATA.xlsx",
                                      {"Data",1,{i}}],{i,MaxDataRow}]];
(* Define functions for retrieving Excel Data *)
        DataVal[row_,column_]  := DataRow[[row,column]];
        ParamRow[mn_]          := Switch[mn, 1, 1, 2,21, 3,41, 4,61];
        ParamColumn[pn_]       := Switch[pn, T, 2, rho, 3,    cp, 4,mu, 5,
                                    nu, 6,  k, 7, alpha, 8,Pr, 9, Grcoeff, 10];
        Parameters[pn_,mn_,T_] := For[i = 1, i <= 19, i++,
                                      PR = ParamRow[mn];
                                      PC = ParamColumn[pn];
                                      NumVal = If[(DataVal[PR + i, 2] <= T) && (T <= DataVal[PR + 1 + i, 2]),
                                                  Return[DataVal[PR + i, PC]],
                                                  NA
                                                ]
                                    ];
(* Retrieve Data *)
        For[i = 1, i <= MaxDataRow, i++, DataRow[[i]] = Data[[1,i]]];



(* STEP 3: CALCULATE MODEL PARAMETERS ---------------------------------------------------------------------------- *)
(* Define functions of physical quantities *)
        DeltaH[T_] := 0;
        FluxAir[q_,FPCM_,FAir_,TPCM_,Tair_] :=
                            q(FPCM^4/5)(FAir^4/5) +
                            (q^(4/5))((FPCM^4/5)Kc* + Kc*(FAir^4/5)) -
                            (FPCM^4/5)*Kc*(FAir^4/5)(TPCM - Tair);
        FluxPipe[q_,FPCM_,TPCM_,Tpipe_] :=
                            q(1/(Kc)) + (q^(4/5)*(1/FPCM)^(4/5)) +
                            Tpipe - TPCM;
(* Temperature *)
        TWater[[1,1]] = Twater;
        TPipe[[1]]    = Tpipe;
        TPCM[[1]]     = Tpcm;
        TAir[[1]]     = Tair;
(* Heat *)
        QWater[[1,1]] = 0;
        QPipe[[1]]    = 0;
        QPCM[[1]]     = WorkSteam; (* Assume insulation is good enough so all stored heat gets to water *)
        QAir[[1]]     = 0;
(* Dimensions *)
        Mass = QPCM[[1]]/HeatOfFusion;
        Volum = Mass/Density;
        WaterPipeOuterDiameter = WaterPipeInnerDiameter + MetalThickness;
        CrossSectionPCM = Volum/L;
        CrossSectionPipes = 2*Pi*(WaterPipeOuterDiameter/2)^2;
        Are = CrossSectionPCM + CrossSectionPipes;
        PCMTankInnerDiameter   = 2*Sqrt[Are/Pi];
        PCMTankOuterDiameter   = PCMTankInnerDiameter + MetalThickness;
        A[[1]] = Pi*PCMTankInnerDiameter*L;
        A[[2]] = Pi*PCMTankOuterDiameter*L;
        A[[3]] = Pi*WaterPipeInnerDiameter*L;
        A[[4]] = Pi*WaterPipeOuterDiameter*L;
        Vol[[1]] = Pi*(PCMTankInnerDiameter/2)^2*L;
        Vol[[2]] = Pi*(PCMTankOuterDiameter/2)^2*L;
        Vol[[3]] = Pi*(WaterPipeInnerDiameter/2)^2*L;
        Vol[[4]] = Pi*(WaterPipeOuterDiameter/2)^2*L;
        CharL[[1]] = Vol[[1]]/A[[1]];
        CharL[[2]] = Vol[[2]]/A[[2]];
        CharL[[3]] = Vol[[3]]/A[[3]];
        CharL[[4]] = Vol[[4]]/A[[4]];



(* STEP 4: DO TEMPERATURE CALCULATIONS ---------------------------------------------------------------------------- *)
(* Time Iteration *)
For[t = 1, t <= tfact, t++,
        tVal[[t + 1]] = time*t;
        For[mn = 1, mn <= 2, mn++,
                (* Retrieve parameters for each material *)
                T = Switch[mn, 1, TAir[[t]], 2, TPCM[[t]] ];
                rho[[mn]]     = Parameters[rho, mn, T];
                cp[[mn]]      = Parameters[cp, mn, T];
                mu[[mn]]      = Parameters[mu, mn, T];
                nu[[mn]]      = Parameters[nu, mn, T];
                k[[mn]]       = Parameters[k, mn, T];
                alpha[[mn]]   = Parameters[alpha, mn, T];
                Pr[[mn]]      = Parameters[Pr, mn, T];
                Grcoeff[[mn]] = Parameters[Grcoeff, mn, T];
                (* Compute coefficients for each material *)
                Gr[[mn]]  = Grcoeff[[mn]]*(A[[mn]]/Pi)^3;
                Ra[[mn]]  = Gr[[mn]]*Pr[[mn]];
                Nu[[mn]]  = 0.54*(Ra[[mn]])^(1/4);
```

```
                h[[mn]]   = Nu[[mn]]*k[[mn]]/CharL[[mn]];
                F[[mn]]   = h[[mn]]*A[[mn]];
        ];
        (* Calculate TAir t + 1 *)
        qair = NSolve[FluxAir[Fluxair, F[[2]], F[[1]], TPCM[[t]], TAir[[t]] ] == 0, Fluxair, Reals];
        qair = Fluxair /. qair;
        QAir[[t + 1]] = First[QAir[[t]] + A[[2]]*qair*time];
        TAir[[t + 1]] = TAir[[t]];
        (* Calculate TPipe t + 1 *)
        qpipe = NSolve[FluxPipe[Fluxpipe, F[[2]], TPCM[[t]], TPipe[[t]] ] == 0, Fluxpipe, Reals];
        qpipe = Fluxpipe /. qpipe;
        QPipe[[t + 1]] = First[QPipe[[t]] + A[[3]]*qpipe*time];
        TPipe[[t + 1]] = TPipe[[t]] + (QPipe[[t + 1]])/(490*7900*(Vol[[4]]-Vol[[3]]));
        (* Calculate TWater t + 1 *)
        (* Length Iteration *)
        For[z = 1, z <= length - 1, z++,
                zVal[[z + 1]] = zfact*z;
                (* Retrieve parameters for each material *)
                mn = 3;
                T = TWater[[z,t]];
                rho[[mn]]     = Parameters[rho, mn, T];
                cp[[mn]]      = Parameters[cp, mn, T];
                mu[[mn]]      = Parameters[mu, mn, T];
                nu[[mn]]      = Parameters[nu, mn, T];
                k[[mn]]       = Parameters[k, mn, T];
                alpha[[mn]]   = Parameters[alpha, mn, T];
                Pr[[mn]]      = Parameters[Pr, mn, T];
                Grcoeff[[mn]] = Parameters[Grcoeff, mn, T];
                (* Compute coefficients for each material *)
                Gr[[mn]]  = Grcoeff[[mn]]*(WaterPipeInnerDiameter)^3;
                Ra[[mn]]  = Gr[[mn]]*Pr[[mn]];
                Nu[[mn]]  = 0.54*(Ra[[mn]])^(1/4);
                h[[mn]]   = Nu[[mn]]*k[[mn]]/CharL[[mn]];
                F[[mn]]   = h[[mn]]*A[[mn]];
                TWater[[z + 1, t]] = N[ TPipe[[t]] + (TWater[[z,t]] - TPipe[[t]])*
                                     Exp[-h[[mn]]*4*zfact/(WaterPipeInnerDiameter*rho[[mn]]*Vf*cp[[mn]])]];
                QWater[[z + 1, t]] = QWater[[z, t]] + rho[[mn]]*(Vol[[3]]/length)*cp[[mn]]*(TWater[[z + 1, t]])
                                     + DeltaH[T];
            ];
        TWater[[1, t + 1]] = TWater[[length, t]] - TDrop;
        QWater[[1, t + 1]] = QWater[[length, t]] - rho[[mn]]*Vol[[3]]*cp[[mn]]*TDrop;
        (* Calculate TPCM t + 1 *)
        TPCM[[t + 1]] = TPCM[[t]];
        QPCM[[t + 1]] = QPCM[[1]] - QAir[[t + 1]] - QPipe[[t + 1]] - QWater[[1, t + 1]];
];


(* STEP 5: RETURN RESULTS ------------------------------------------------------------------------------------------ *)
        (* Variables *)
        MaxEfficiency;
        zVal;
        tVal;
        Mass;
        Volum;
        (* Parameter Table *)
        PM[[1,1]] = "Time";
        PM[[1,3]] = "TWater";
        PM[[1,5]] = "TPipe";
        PM[[1,7]] = "QWater";
        PM[[1,9]] = "QPipe";
        PM[[1,11]] = "QPCM";
        PM[[1,13]] = "QAir";
        PM[[1,15]] = "QTotal";
        For[j = 1, j <= tfact + 1, j++,
                PM[[ j,2]] = tVal[[j]];
                PM[[ j,4]] = TWater[[1,j]];
                PM[[ j,6]] = TPipe[[j]];
                PM[[ j,8]] = QWater[[1,j]];
                PM[[ j,10]] = QPipe[[j]];
                PM[[ j,12]] = QPCM[[j]];
                PM[[ j,14]] = QAir[[j]];
                PM[[ j,16]] = QAir[[j]] + QPCM[[j]] + QPipe[[j]] + QWater[[1,j]];
        ]
        (* Plots *)
        ListPlot[Table[{tVal[[i]],TWater[[1,i]]},{i,1,tfact + 1}],
                 AxesLabel -> {"Time (s)","Water Temperature (K)"},
                 PlotLabel -> "Water temperature change" ]
        ListLinePlot[Table[{tVal[[k]], PM[[k,p]]}, {p, {8,10,12,14,16}}, {k, 1, tfact + 1}],
                PlotLegends -> {Water, Pipe, PCM, Air, Total},
                AxesLabel -> {"Time (s)","Heat (J)"},
                PlotLabel -> "Energy Balance"]
        PM //MatrixForm;
```

Excel Model Data (taken from Heat Transfer textbook [52], SI units)

Air	Temp	rho	cp	mu	nu	k	alpha	Pr	Grcoeff
	1	1000	1000	1000	1000	1000	1000	1000	1000
	280	1.2614	1.0057	1.7503	1.3876	2.4671	1.9448	0.713	1.815
	300	1.1769	1.0063	1.8464	1.5689	2.624	2.2156	0.708	1.327
	320	1.1032	1.0073	1.9391	1.7577	2.7785	2.5003	0.703	0.9942
	340	1.0382	1.0085	2.03	1.9553	2.9282	2.7967	0.699	0.7502
	360	0.9805	1.01	2.1175	2.1596	3.0779	3.108	0.695	0.5828
	400	0.8822	1.0142	2.2857	2.5909	3.3651	3.761	0.689	0.3656
	440	0.8021	1.0197	2.4453	3.0486	3.6427	4.4537	0.684	0.2394
	480	0.7351	1.0263	2.5963	3.5319	3.9107	5.1836	0.681	0.1627
	520	0.6786	1.0339	2.7422	4.041	4.169	5.9421	0.68	0.1156
	580	0.6084	1.0468	2.9515	4.8512	4.5407	7.1297	0.68	7193000
	700	0.504	1.0751	3.3325	6.6121	5.236	9.6632	0.684	3.21
	2000	1000	1000	1000	1000	1000	1000	1000	1000
	1	1000	1000	1000	1000	1000	1000	1000	1000
	1	1000	1000	1000	1000	1000	1000	1000	1000
	1	1000	1000	1000	1000	1000	1000	1000	1000
	1	1000	1000	1000	1000	1000	1000	1000	1000
	1	1000	1000	1000	1000	1000	1000	1000	1000
	1	1000	1000	1000	1000	1000	1000	1000	1000

Water	Temp	rho	cp	mu	nu	k	alpha	Pr	Grcoeff
	1	1000	1000	1000	1000	1000	1000	1000	1000
	273	999.3	4226	1794	1.795	0.558	0.132	13.6	1
	293	998.2	4182	993	0.995	0.597	0.143	6.96	2.035
	313	992.2	4175	658	0.663	0.633	0.153	4.33	8.833
	333	983.2	4181	472	0.48	0.658	0.16	3	22.75
	353	971.8	4194	352	0.362	0.673	0.165	2.57	46.68
	373	958.4	4211	278	0.29	0.682	0.169	1.72	85.09
	473	862.8	4501	139	0.161	0.665	0.171	0.94	517.2
	573	712.5	5694	92.2	0.129	0.564	0.139	0.93	1766
	600	0.3667	2.0264	20.64	5.6286	4.2161	5.6738	0.992	0.5154
	650	0.3383	2.0555	22.45	6.6361	4.6361	6.667	0.995	0.3415
	700	0.314	2.0869	24.25	7.7229	5.0593	7.7207	1	0.2277
	750	0.293	2.1192	26.06	8.8942	5.4841	8.8321	1.007	0.1651
	800	0.2746	2.1529	27.86	10.1457	5.9089	9.995	1.015	0.1183
	2000	1000	1000	1000	1000	1000	1000	1000	1000
	1	1000	1000	1000	1000	1000	1000	1000	1000
	1	1000	1000	1000	1000	1000	1000	1000	1000
	1	1000	1000	1000	1000	1000	1000	1000	1000
	1	1000	1000	1000	1000	1000	1000	1000	1000

PCM	Temp	rho	cp	mu	nu	k	alpha	Pr	Grcoeff
	1	1000	1000	1000	1.00E+0	1000	1.00E+0	1000	1000
	400	2009.24	1464.84	0.01107	5.51E-0	0.04558	1.55E-0	355.754	1725641
	425	1993.34	1469.14	0.00946	4.75E-0	0.04088	1.40E-0	340.253	2322419
	450	1977.44	1473.44	0.00806	4.08E-0	0.03652	1.25E-0	325.395	3148666
	475	1961.54	1477.74	0.00685	3.49E-0	0.03251	1.12E-0	311.507	4292334
	500	1945.64	1482.04	0.00581	2.99E-0	0.02881	9.99E-0	299.004	5866909
	525	1929.74	1486.34	0.00493	2.56E-0	0.02543	8.87E-0	288.406	8007799
	550	1913.84	1490.64	0.00420	2.20E-0	0.02235	7.84E-0	280.367	1085479
	575	1897.94	1494.94	0.00360	1.90E-0	0.01955	6.89E-0	275.700	1451118
	600	1882.04	1499.24	0.00312	1.66E-0	0.01702	6.03E-0	275.412	1897531
	625	1866.14	1503.54	0.00275	1.48E-0	0.01474	5.26E-0	280.735	2406058
	650	1850.24	1507.84	0.00247	1.34E-0	0.01271	4.56E-0	293.149	2935287
	675	1834.34	1512.14	0.00226	1.24E-0	0.01090	3.93E-0	314.392	3427073
	700	1818.44	1516.44	0.00212	1.17E-0	0.00931	3.38E-0	346.412	3824665
	725	1802.54	1520.74	0.00203	1.13E-0	0.00792	2.89E-0	391.250	4094686
	750	1786.64	1525.04	0.00198	1.11E-0	0.00672	2.47E-0	450.753	4239339
	775	1770.74	1529.34	0.00195	1.10E-0	0.00568	2.10E-0	526.046	4292715
	800	1754.84	1533.64	0.00193	1.10E-0	0.00481	1.79E-0	616.635	4307614
	2000	1000	1000	1000	1.00E+0	1000	1.00E+0	1000	1000

Steam	Temp	rho	cp	mu	nu	k	alpha	Pr	Grcoeff
	1	1000	1000	1000	1000	1000	1000	1000	1000
	380	0.586	2.0592	12.7	2.1672	2.452	2.032	1.067	5521000
	400	0.5549	2.0098	13.42	2.4185	2.601	2.3322	1.037	4.1951
	450	0.4911	1.9771	15.23	3.1012	2.9877	3.0771	1.008	2.2558
	500	0.441	1.9817	17.03	3.8617	3.3903	3.8794	0.995	1.3139
	550	0.4004	2.0006	18.84	4.7053	3.8008	4.7448	0.992	0.8069
	600	0.3667	2.0264	20.64	5.6286	4.2161	5.6738	0.992	0.5154
	650	0.3383	2.0555	22.45	6.6361	4.6361	6.667	0.995	0.3415
	700	0.314	2.0869	24.25	7.7229	5.0593	7.7207	1	0.2277
	750	0.293	2.1192	26.06	8.8942	5.4841	8.8321	1.007	0.1651
	800	0.2746	2.1529	27.86	10.1457	5.9089	9.995	1.015	0.1183
	2000	1000	1000	1000	1000	1000	1000	1000	1000
	1	1000	1000	1000	1000	1000	1000	1000	1000
	1	1000	1000	1000	1000	1000	1000	1000	1000
	1	1000	1000	1000	1000	1000	1000	1000	1000
	1	1000	1000	1000	1000	1000	1000	1000	1000
	1	1000	1000	1000	1000	1000	1000	1000	1000
	1	1000	1000	1000	1000	1000	1000	1000	1000
	1	1000	1000	1000	1000	1000	1000	1000	1000

Note on Figure 4:

Unfortunately, for some reason beyond my comprehension, I could not get the graphs to work correctly. Maximum temperature should be reached at the end of the time period. On the first graph, the behavior of the temperature increase should mimic the exponential nature of Equation 6. The Energy graph is also not completely accurate: The PCM Energy (green line) should reach 0 at t = 3600 s in order to ensure a power dissipation of 2.5MW in 1 hr.

- Federico Poggioli.

APPENDIX B: HEAT LOSS EXCEL SPREADSHEET

TESM Properties								
Kinematic Viscosity (Pa*s)	Cp (kJ/(kg*K)	Thermal Conductivity (fluid) (W/(m*	Thermal Expansion Coefficient (1/K)	Density (kg/m^3)	Melting Point (deg C)	Ra	Nu	h (W/(m*K))
2.63	1.22	0.5	3.78	2110	330	689112	16.999	1.133269641
Air Properties								
Kinematic Viscosity (Pa*s)	Cp (kJ/(kg*K))	Thermal Conductivity (W/(m*K))	Thermal Expansion Coefficient (1/K)	Density (kg/m^3)	Functioning Temp (deg	Ra	Nu	h (W/(m*K))
0.0000186	1	0.02624	0.0034	1.225	25	9.6E+13	1845.1	6.455300901
Insulation Properties								
	Thickness (m)	Thermal Conductivity (W/(m*K))						
	1	0.1						
Container Properties								
Height (m)	Diameter (m)	Volume (m^3)	Inner Surface Area (m^2)	Capacity (kJ)				
7.5	1.65	16.03684875	43.15370209	9000000				
				Capacity (kWh)				
Calculated Values				2500				
Heat Flux (W/m^2)	Q (W)	%loss/hr						
27.63353481	1192.489329	0.047699573						

APPENDIX C: PYTHON PROGRAM FOR MARKET ANALYSIS

```
import numpy as np
import csv
import pandas as pd
import matplotlib.pyplot as mtplt
import matplotlib.patches as mpatches
from matplotlib.widgets import TextBox
import os, sys, codecs
from scipy.signal import argrelextrema
import scipy.integrate
from datetime import datetime
import locale

#481 lines per day of data (last data point is next set's first data point)

efficiency = .40                        #cycle efficiency
efficiencyLoss = .00047                 #stored %energy lost per hour
storage = 2500                          #in kWh
peakCost = (1.618+2.31+1+.5)*.01        #$/kWh
offPeakCost = (.865+2.31+1+.5)*.01      #$/kWh
month = 'October'


def remove_bom_inplace(path):
   """Removes BOM mark, if it exists, from a file and rewrites it in-place"""
   buffer_size = 4096
   bom_length = len(codecs.BOM_UTF8)

   with open(path, "r+b") as fp:
       chunk = fp.read(buffer_size)
       if chunk.startswith(codecs.BOM_UTF8):
           i = 0
           chunk = chunk[bom_length:]
           while chunk:
               fp.seek(i)
               fp.write(chunk)
               i += len(chunk)
               fp.seek(bom_length, os.SEEK_CUR)
               chunk = fp.read(buffer_size)
           fp.seek(-bom_length, os.SEEK_CUR)
           fp.truncate()


##remove_bom_inplace(filename + '.csv')

##data = np.loadtxt(fname=filename + '.csv', delimiter=',')

def averageDayLoad():
   # filename = 'HCl Diluted Fluorescence Spectrum'
   # demandArray = [[]]
   #
   # for n in range(31):
    #      demandArray.append(pd.read_csv('./DemandCSV (' + str(n+1) + ')/Demand (' + str(n+1) +
').csv', index_col=0))
   # print (demandArray)

   dataSetLoad = []
   setPoint = 0
   workingData = []
```

```
    for n in range(31):
        with open ('./' + month +'/DemandCSV (' + str(n+1) + ')/Demand (' + str(n+1) + ').csv') as
data:
            data = csv.reader(data, delimiter = ',')
            for row in data:
                workingData.append(row)

    for n in range(480):

        for day in range (31):
            setPoint += float(workingData[n+481*day][2])

        dataSetLoad.append(setPoint/31)
        setPoint = 0

    print(dataSetLoad)
    print(dataSetLoad.__len__())

    return (dataSetLoad)

def loadTimes():
    locale.setlocale(locale.LC_ALL, 'en_US')
    tempSetTimes = []
    dataSetTimes = []
    workingData = []

    for n in range(31):
            with open('./' + month + '/DemandCSV (' + str(n + 1) + ')/Demand (' + str(n + 1) +
').csv') as data:
            data = csv.reader(data, delimiter=',')
            for row in data:
                workingData.append(row)

    for n in range(480):
        tempSetTimes.append(workingData[n][0])

    for n in range (480):
        tempSetTimes[n] = tempSetTimes[n].replace('EDT', 'GMT')

    for n in range(480):

        dataSetTimes.append(datetime.strptime(tempSetTimes[n], '%m/%d/%Y %I:%M:%S %p %Z'))

    for n in range(480):
        dataSetTimes[n] = dataSetTimes[n].time()

    print(dataSetTimes)
    print(dataSetTimes.__len__())

    return (dataSetTimes)


def averageDayPrice():
    # filename = 'HCl Diluted Fluorescence Spectrum'
    # demandArray = [[]]
    #
    # for n in range(31):
     #      demandArray.append(pd.read_csv('./DemandCSV (' + str(n+1) + ')/Demand (' + str(n+1) +
').csv', index_col=0))
    # print (demandArray)

    dataSetPrices = []
    setPoint = 0
    workingData = []
```

```
    for n in range(31):
        with open ('./' + month +'/RTData (' + str(n+1) + ')' + '.csv') as data:
            data = csv.reader(data, delimiter = ',')
            for row in data:
                workingData.append(row)

    for n in range(287):

        for day in range (31):
            setPoint += float(workingData[n+287*day][3])

        dataSetPrices.append(setPoint/(31*1000) + (2.31+1+.5)*.01)
        setPoint = 0

    print(dataSetPrices)
    print(dataSetPrices.__len__())


    return (dataSetPrices)

def averageDayLoad():
    # filename = 'HCl Diluted Fluorescence Spectrum'
    # demandArray = [[]]
    #
    # for n in range(31):
     #       demandArray.append(pd.read_csv('./DemandCSV (' + str(n+1) + ')/Demand (' + str(n+1) +
').csv', index_col=0))
    # print (demandArray)

    dataSetLoad = []
    setPoint = 0
    workingData = []

    for n in range(31):
         with open ('./' + month +'/DemandCSV (' + str(n+1) + ')/Demand (' + str(n+1) + ').csv') as
data:
            data = csv.reader(data, delimiter = ',')
            for row in data:
                workingData.append(row)

    for n in range(480):

        for day in range (31):
            setPoint += float(workingData[n+481*day][2])

        dataSetLoad.append(setPoint/31)
        setPoint = 0

    print(dataSetLoad)
    print(dataSetLoad.__len__())


    return (dataSetLoad)

def loadTimes():
    locale.setlocale(locale.LC_ALL, 'en_US')
    tempSetTimes = []
    dataSetTimes = []
    workingData = []

    for n in range(31):
            with open('./' + month + '/DemandCSV (' + str(n + 1) + ')/Demand (' + str(n + 1) +
').csv') as data:
            data = csv.reader(data, delimiter=',')
            for row in data:
                workingData.append(row)
```

```
    for n in range(480):
        tempSetTimes.append(workingData[n][0])

    for n in range (480):
        tempSetTimes[n] = tempSetTimes[n].replace('EDT', 'GMT')

    for n in range(480):

        dataSetTimes.append(datetime.strptime(tempSetTimes[n], '%m/%d/%Y %I:%M:%S %p %Z'))

    for n in range(480):
        dataSetTimes[n] = dataSetTimes[n].time()

    print(dataSetTimes)
    print(dataSetTimes.__len__())

    return (dataSetTimes)

x = loadTimes()
y = averageDayLoad()
xInHours = []

for value in range (480):
    xInHours.append(value*.05)

def priceTimes():
    locale.setlocale(locale.LC_ALL, 'en_US')
    tempSetTimes = []
    dataSetTimes = []
    workingData = []

    for n in range(31):
        with open('./' + month + '/RTData (' + str(n+1) + ')' + '.csv') as data:
            data = csv.reader(data, delimiter=',')
            for row in data:
                workingData.append(row)

    for n in range(287):
        tempSetTimes.append(workingData[n][0])

    for n in range (287):
        tempSetTimes[n] = tempSetTimes[n].replace('EDT', 'GMT')

    for n in range(287):

        dataSetTimes.append(datetime.strptime(tempSetTimes[n], '%m/%d/%Y %H:%M'))

    for n in range(287):
        dataSetTimes[n] = dataSetTimes[n].time()

    print(dataSetTimes)
    print(dataSetTimes.__len__())

    return (dataSetTimes)

def storageStartTime(capacity):

    for i in range(161,0, -1):
        #print('INDEX: ' + str(i))
        if np.trapz(y[i:161], xInHours[i:161]) > storage:
            # print(np.trapz(y[i:161], xInHours[i:161]))
            # print(x[i])
            return int(i)
            print(i)
            break
```

```
def dischargeEndTime(e, capacity):
   for i in range(161,480):
       if np.trapz(y[161:i],xInHours[161:i]) > (capacity * e):
           # print(np.trapz(y[161:i],xInHours[161:i]))
           # print(x[i])
           return int(i)
           print (i)
           break

def chargeCost():
   print(np.trapz(y[:161], xInHours[:161]))
                                                            return                    storage*offPeakCost
#(np.trapz(y[storageStartTime(storage):161],xInHours[storageStartTime(storage):161])*offPeakCost)

def dischargeCost():
                  print((float((float(np.trapz(y[161:dischargeEndTime(efficiency,      storage)],
xInHours[161:dischargeEndTime(efficiency,storage)]))                                                    -
((float(xInHours[dischargeEndTime(efficiency,storage)])-xInHours[storageStartTime(storage)])*stor
age*efficiencyLoss))) * float(peakCost)))
                                                                                                     return
storage*efficiency*peakCost#(float((float(np.trapz(y[161:dischargeEndTime(efficiency,storage)],
xInHours[161:dischargeEndTime(efficiency,storage)]))                                                    -
((float(xInHours[dischargeEndTime(efficiency,storage)])-xInHours[storageStartTime(storage)])*stor
age*efficiencyLoss))) * float(peakCost))

def profits():
   return dischargeCost()-chargeCost()

def profitsToGraph(e, capacity):
   sStart = (storageStartTime(capacity))
   dEnd = (dischargeEndTime(e,capacity))

   chargeCost = capacity * offPeakCost

   dischargeCost = capacity*e*peakCost

   return dischargeCost-chargeCost


def peakTime():
   maxIndex = (np.argmax(y))
   return (x[maxIndex])

def troughTime():
   minIndex = (np.argmin(y))
   return (x[minIndex])

def peakConsumption(y):
   return y[np.argmax(y)]

def troughConsumption(y):
   return y[np.argmin(y)]

def arrayAverage(y):
   return np.mean(y)

x = priceTimes()
y = averageDayPrice()
xInHours = []

# for val in range(len(y)):
#     if y[val] < arrayAverage(y):
#         val
```

```
# for value in range (480):
#     xInHours.append(value*.05)


# mtplt.text(x[8], .069 , 'Peak Price: ' + str(round(peakConsumption(averageDayPrice()),4)) + '
$/kWh')
# mtplt.text(x[8], .0675 , 'Trough Price: ' + str(round(troughConsumption(averageDayPrice()),4))
+ ' $/kWh')
# mtplt.text(x[8], .066 , 'Trough/Peak Price Ratio: ' +
str(round(troughConsumption(averageDayPrice())/peakConsumption(averageDayPrice()),3)))
# mtplt.text(x[8], .0645 , 'Average Price: ' + str(round(arrayAverage(y),3)) + ' $/kWh')

# mtplt.text(x[8], .0745 , 'Average Price: ' + str(troughTime()) + ' $/kWh')
# mtplt.text(x[8], .0765 , 'Average Price: ' + str(peakTime()) )

# sStart = (storageStartTime(storage))
# # dEnd = (dischargeEndTime(.1,storage))
# # print ('hello' + str(xInHours[dEnd] - xInHours[sStart]))
#
# # mtplt.text(x[10], 1980 , 'Peak Consumption (' + str(int(peakConsumption())) + ' kW) @' +
str(peakTime()))
# # mtplt.text(x[10], 1870, 'Trough Consumption (' + str(int(troughConsumption())) + ' kW) @' +
str(troughTime()))
# # mtplt.text(x[10], 1980 , 'Charging Times: ' + str(x[storageStartTime(storage)]) + ' to ' +
str(x[161]) + '@~1000kW draw')
# # mtplt.text(x[10], 1870, 'Discharging Times: ' + str(x[161]) + ' to ' +
str(x[dischargeEndTime(efficiency, storage)]))
# mtplt.text(x[10], 2020 , 'Charging Cost: $' + str('%.2f'%(chargeCost())))
# mtplt.text(x[10], 1920, 'Discharging Profit: $' + str('%.2f'%(dischargeCost())))
# mtplt.text(x[10], 1820, 'Net Profit Per Day: $' + str('%.2f'%(profits())))
# # mtplt.text(.01, 17, 'Minimum storage efficiency for profit each day: ' +
str(100*efficiencyProfitThreshold) + '%')
#
# #
# #
# mtplt.fill_between(x[:161],y[:161],0, color = "green", alpha = .3)
# mtplt.fill_between(x[161:421],y[161:421],0, color = "red", alpha = .3)
# mtplt.fill_between(x[421:],y[421:],0, color = "green", alpha = .3)
# #
# mtplt.plot(peakTime(), peakConsumption(), 'ro', color = 'blue')
# mtplt.plot(troughTime(), troughConsumption(), 'ro', color = 'blue')
# #
# # mtplt.title('Average ' + month + ' Day Power Consumption')
# mtplt.title('Average ' + month + ' 2.5 MWh (1 MWh Effective Storage) Thermal Battery Charge and
Discharge Cycles')
# # mtplt.title('Profit Over Iterated Storage Efficiency In Lithium-Ion Battery @Capacity of ' +
str(storage) + 'kWh')
# mtplt.ylabel('Consumption (kW)')
# mtplt.xlabel('Time')

mtplt.title('Real Time Electricity Pricing Over ' + month)
mtplt.ylabel('Energy Cost($/kWh)')
mtplt.xlabel('Time')

mtplt.xlim(xmin = 0, xmax = x[286])
# mtplt.ylim(ymax = .1)

print(np.percentile(y,0))

mtplt.plot(x,y)
mtplt.show()
```